1955

The photometric measurement of droplet size

Baker, Charles F.

Massachusetts Institute of Technology

http://hdl.handle.net/10945/14496

THE PHOTOMETRIC MEASUREMENT OF DROPLET SIZE

Charles Frederick Baker
and
James Hamilton Webber

1-2

PHO — PHOTOMETER
MEA — MEASUREMENT
DRO — DROPLETS

Letter on cover:

THE PHOTOMETRIC MEASUREMENT OF
DROPLET SIZE

Charles Fredrick Baker

and

James Hamilton Wehler

THE PHOTOMETRIC MEASUREMENT OF DROPLET SIZE

by

Charles Fredrick Baker
B.S., U.S. Coast Guard Academy
(1946)

and

James Hamilton Webber
B.S., U.S. Naval Academy
(1949)
S.M., Massachusetts Institute of Technology
(1955)

SUBMITTED IN PARTIAL FULFILLMENT OF THE
REQUIREMENTS FOR THE DEGREE OF
NAVAL ENGINEER

at the

MASSACHUSETTS INSTITUTE OF TECHNOLOGY
June 1955

Signatures of Authors ....

....

Certified by ....
Thesis Supervisor

Accepted by ....
Chairman of Departmental Committee on Graduate Students

ACKNOWLEDGEMENTS

In concluding this thesis it is a pleasure to express our gratitude to those people who have contributed to the development of the project.

The wise counsel of Professor A. H. Shapiro has exerted a steadying influence throughout, and many times has directed our efforts along paths which later proved to be fruitful. As thesis supervisor, Professor K. R. Wadleigh gave his time freely and was a constant source of advice and encouragement in many perplexing situations.

We are especially indebted to Professors F. W. Sears of M. I. T. and J. C. Johnson of Worcester Polytechnic Institute who provided much of the background information on the fundamentals of optics and light scattering. The patience of both of these persons in dealing with two novices in the field is particularly appreciated.

Thanks are also due the W. M. Welch Manufacturing Company for the use of their excellent instrument, the Densichron. Miss Margaret Tefft contributed ably in the secretarial work.

33917

THE PHOTOMETRIC MEASUREMENT OF DROPLET SIZE

by

Charles Fredrick Baker

and

James Hamilton Webber

Submitted to the Department of Naval Architecture and Marine Engineering on May 23, 1955 in partial fulfillment of the requirements for the degree of Naval Engineer.

ABSTRACT

The Mie theory of light scattering by spherical particles is reviewed. This theory shows that the scattering area coefficient, the ratio of scattering cross section to the geometric cross section, is about 2.0 for particles whose diameter is large compared with the wave length of the incident light. The scattered light has two components, that intercepted by the particle and scattered equally in all directions, and that which is diffracted by the edge of the particle. When the particle size is large, the two components are about equal in magnitude; however, the diffracted light is contained within a very small solid angle ahead of the particle. In order that a given optical system will actually observe a scattering area of about 2.0, it is necessary to exclude all of the diffracted light from the photocell which records the intensity of the transmitted light.

An approximate analysis is advanced to predict the percentage of diffracted light which can be segregated from the transmitted parallel light as a function of the "cone of observation". An optical system for filtering out most of the diffracted light from the parallel light is proposed. The approximate analysis of this optical system, coupled with the angular distribution pattern of the diffracted light provide the basis for the rational design of a forward scattering photometer.

Experimental photometric data measuring the diffraction of monochromatic light by 26.6 and 30.1 micron glass beads suspended in oil has verified the approximate theories advanced. The correlation of the experimental results with the theoretical predictions is considered excellent. Initial calibration runs

were made on a system in which glass beads were carried past the photometer by a high speed air stream, however time did not permit the successful completion of this calibration. It is recommended that a full investigation of the dynamic calibration apparatus be launched with the object of completely defining the flow conditions. When this is sufficiently understood, the photometer should provide quick and convenient measurements of droplet size in studies of atomization.

Thesis Supervisor: K. R. Wadleigh

Title: Associate Professor of Mechanical Engineering

TABLE OF CONTENTS

LIST OF FIGURES

LIST OF SYMBOLS

a	radius of droplet or particle (microns)
$a_{\frac{3}{2}}$	volume-surface mean radius (microns)
A	cross-sectional area of flow (ft^2)
c	distance from aerosol or individual droplet to first focal point of collecting lens. See Figure VIII.
d	diameter of droplet or particle (microns)
$d_{\frac{3}{2}}$	volume-surface mean diameter (microns)
D	optical density as read from Densichron log scale. $D = \log_{10} 1/E$
E	flux density = flux divided by area ($watts/meter^2$)
E_o	flux density of parallel radiation incident on the plane of the droplet
f	focal length of a lens
F	flux = total power passing through a surface perpendicular to the power flow (watts)
G	distribution function = dn/da
h	enthalpy (BTU/lb)
h_o	stagnation enthalpy (BTU/lb)
I	intensity of radiation = flux per unit solid angle (watts/steradian)
I_D	intensity of diffracted radiation
i_D	relative intensity = I_D/I_o
J_1	Bessel function of the first order
k	absorption index, also the ratio of specific heats
l	light path length in an aerosol
K_s	scattering area coefficient, $K_s = S/\pi a^2$
K_{so}	observed scattering area coefficient

m	index of refraction of the droplet relative to that of the surrounding medium
M	Mach Number, ratio of velocity to the local velocity of sound
n	number of particles per unit volume of an aerosol
p	static pressure (lb/ft^2)
p_o	stagnation pressure (lb/ft^2)
r	radius of aperture
r'	radius of diffraction pattern from a single drop, in the plane of the collecting lens
R	radius of light beam incident on the plane of the collecting lens
S	total scattering cross-section for a spherical particle
w	weight of particles in a volume V of the medium (gm)
w_a	mass rate of flow of air (lb/sec)
w_b	mass rate of flow of particles (lb/sec)
W	weight of oil in which glass beads were suspended (gm)
V	volume of medium containing aerosol particles or water droplets (cm^3); also velocity (ft/sec)
T	temperature, ^{o}R.
T_o	stagnation temperature, ^{o}R.
α	dimensionless parameter = $2\pi a/\lambda$
β	dimensionless parameter = $\frac{\alpha}{2} \sin \theta$
λ	wave length of radiation (microns)
θ	angle of observation measured from the direction of the incident radiation
ψ	angle of observation measured from the direction of the incident light, which is actually observed by a photometric apparatus
ω	solid angle = any area projected on a sphere of radius L divided by the square of this radius (steradians)

SECTION I

Introduction

In the Aerothermopressor, water is sprayed into a hot, high velocity gas stream in an attempt to obtain the stagnation pressure rise which the theory predicts. (See Shapiro, et al, (29)* for a complete discussion of the Aerothermopressor.) Theoretical considerations indicate that the most important requirement for effective performance of the Aerothermopressor is an atomization system that will produce very small water droplets. In attempting to reproduce theoretically the complex phenomena which occur within the Aerothermopressor, it has become evident that accurate predictions of water droplet size are essential.

The present state of knowledge on the mechanism of atomization of a liquid sprayed into a high velocity gas stream is severely limited by the sparcity of experimental data. In order that precise data may be obtained, it is necessary to have some method of measuring droplet size. It is to fill this need that the photometric apparatus described herein has been developed.

At the present time the theoretical calculations for the Aerothermopressor assume an initial drop diameter calculated by the Nukiyama and Tanasawa formula (27). No atomization experiments are being conducted at present because of the lack of suitable drop size measuring methods.

Previous investigations associated with the Aerothermopressor development have indicated that only two methods of measuring water

---

* Numbers in parentheses refer to references listed in Appendix I, Bibliography

droplet size in a high velocity gas stream are feasible. One method employs an impact probe described by Keeler (17). Research is continuing at present on this method. The other is the photometric method described in this thesis. Previous research on the photometric method has been conducted by Cheatham (3) and McGrew (24). Numerous other techniques have been employed by various investigators to determine droplet size. Many of these techniques have been investigated and evaluated by Kesler (20). In general, however, the other techniques are not adaptable to the measurement of droplets in a hot, high velocity gas stream. On the other hand, the photometric method appears particularly well suited for such measurements because the required data can be obtained without disturbing the flow pattern; the procedure yields directly the volume-surface mean diameter of the droplet spectrum; and the instrumentation can conceivably be arranged to provide continuous recording. Limitations of the photometric method, as presented here, are twofold. First, the method yields no information on the droplet spectrum, and second, the measurements are valid only over the size range of about 5 to 50 microns diameter.

The principle of the photometric method is based on the phenomenon of the scattering of light by spherical particles which was developed by G. Mie early in the Twentieth century. This theory is based on the exact solutions of Maxwell's equations for a particle of any material and size. A complete treatment of the theory is presented in a compact form by Stratton (34). The important results of the theory are presented and explained by Sinclair (7,30,32).

Considerable interest has been displayed in the Mie theory in the past twenty years. Many theoretical, experimental and numerical papers have appeared in the literature during this time. Furthermore, the theory has been verified by extensive experimental work. (21)

The Mie theory gives the scattering cross section of a sphere of any size (the total light energy scattered per second per unit intensity of illumination) in the form

$$S = \frac{\lambda^2}{2\pi} \sum_{n=1}^{\infty} (2n+1)\left(|a_n|^2 + |p_n|^2\right) \tag{1}$$

where $|a_n|$ and $|p_n|$ are complex functions of the parameter $\alpha = \frac{2\pi a}{\lambda}$ and the index of refraction, m, of the sphere relative to the surrounding medium. For a droplet, the scattering area coefficient, K_s, has been defined as the ratio of the scattering cross section to the geometric cross section, thus

$$K_s \equiv \frac{S}{\pi a^2} \tag{2}$$

The form of equation (1) is an infinite series of terms in half-order cylindrical functions. As the value of the parameter α increases, the series converges more and more slowly. The efforts of numerous investigators to calculate S forms an interesting part of the history of light scattering investigations. Still other investigators derived approximate equations for S, and Jobst (14) derived an asymptotic expression for S when α becomes large. (The interested reader is referred to references 8, 9, 11, 12, 14, 15, 18, 19, 32 and 36 for further information on numerical and experimental methods employed to determine S and K_s.)

The numerical problems associated with the Mie equations have been lessened a considerable amount by the recent publication of Tables of Light Scattering Functions for Spherical Particles by Gumsprecht and Sliepcevich (6). These tables are based on the solutions of the Mie equations, computations having been made on a high-speed electronic computer. The scattering area coefficient has been computed for various values of the index of refraction ranging from 1.20 to 1.60. Values of K_s for α ranging from 1 to 400 are given. These tables greatly extended the range for which the value of K_s was known as a function of α. Figure I is a plot of K_s versus α for $m = 1.33$ (the index of refraction of water droplets relative to air). For values of α greater than 25, the curve is approximated from the data given in the tables. For α less than 25, the data is taken from Houghton (12), which was more extensive in this region than the data in the tables.

Johnson (16) has shown that K_s is relatively insensitive to the index of absorption when α is greater than about 40; hence, Figure I represents K_s versus α for absorbing as well as transparent particles when α is large.

Figure I also shows that the value of K_s is about 2.0 when α is greater than about 50. From the definition of scattering area coefficient, equation (2), it is seen that this means the scattering cross section is about twice the geometric cross section of the particle as α becomes large. The tables of light scattering functions show this holds for any of the values of the index of refraction which were calculated. The physical concept of why the scattering

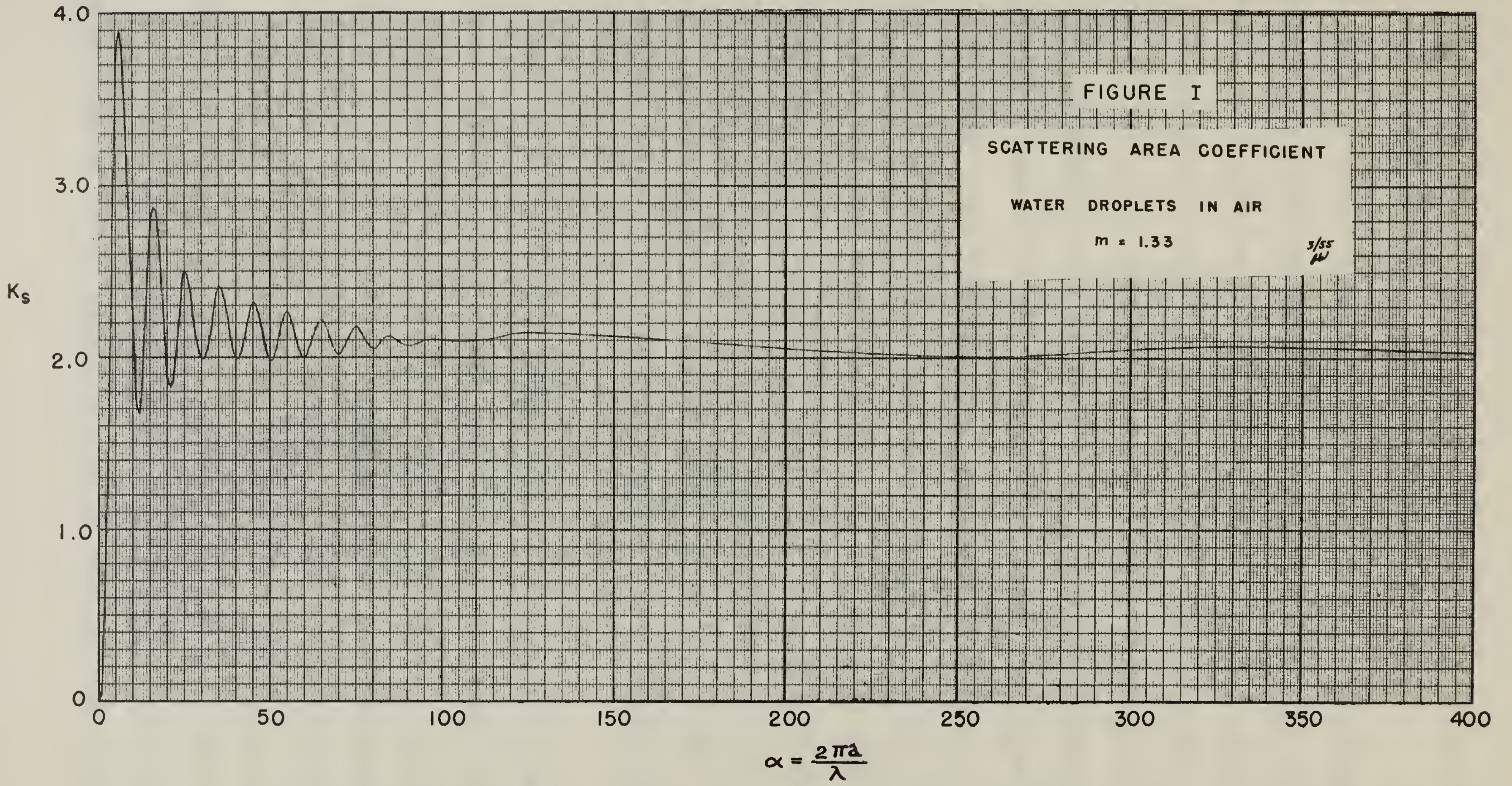

FIGURE I

SCATTERING AREA COEFFICIENT

WATER DROPLETS IN AIR

$m = 1.33$

cross section should be about twice the geometric cross section for large values of α has been given by Sinclair (32).

The light rays directly intercepted by the geometric cross-section of the particle are reflected and refracted through large angles. Moreover, an equal amount of light is diffracted by the edge of the sphere , according to Babinet's principle, which states that diffraction from a circular aperture shows the same diffraction pattern as that from an opaque disc or sphere of the same diameter (16). Thus, the scattering cross-section is equal to twice the geometric cross-section. If this line of reasoning were strictly true, K_s would be exactly equal to 2.0. However, the values of K_s given by Gumprecht show this is true only for large values of α , and then only approximately so. In atomization studies it is anticipated that droplet sizes will range from 5 to 50 microns, which, for blue light ($\lambda = .4\mu$),corresponds to values of α from 40 to 400. These α's are reasonably well within the range where K_s is approximately 2.

When the value of α is large, almost all of the diffracted light is contained within a very small solid angle ahead of the particle. It is, therefore, a difficult problem to observe experimentally a value of K_s near the actual value when the particles are large compared with the wave length because of the difficulty of separating the diffracted light from the transmitted parallel beam. The experimental research of Cheatham (3) was devoted primarily to this problem. He showed that it was indeed possible to have an optical system arranged which would separate nearly all of the diffracted

light from the transmitted beam, thus enabling one to observe a value of K_s which was about equal to its actual value.

In extending the research of Cheatham, it was felt desirable to develop a theory which would permit analysis of a forward-scattering photometer. The theory, analysis, design, calibration and evaluation of the forward-scattering photometer devised is described in the remaining sections of this thesis.

SECTION II

Theoretical Considerations for Design of a Photometer

The Mie theory of light scattering by spherical particles has been used in the development of several different types of photometers to measure particle size and/ or concentration in an aerosol. Each type is generally based on the measurement of one or more of the light scattering functions which vary with particle size. The methods have been successful for aerosols composed of uniform-sized particles when the particle diameter is not much greater than the wave length of the light employed. (See references 4, 7, 21, 23, 26, 30, 31). However, for aerosols composed of non-uniform sized particles the measurement methods have not met with much success. The ultimate hope of investigators is to develop a method which will yield the distribution curve for the aerosol particles. Sinclair (31) does not believe that this will be achieved; however, a method has been investigated with apparent success by the Meteorology Department of the Massachusetts Institute of Technology to determine droplet size distribution and water content of clouds (15, 18, 19). The method investigated here is somewhat less ambitious, since its purpose is to yield the volume-surface mean radius of the droplets atomized by a high speed air stream. In contrast to the photometers previously developed, the present instrument should be able to determine the mean size of water droplets in a non-uniform aerosol, where the droplet diameter is considerably greater than the wave length of the light. The method is based

on measuring the total scattering produced by the droplets; the instrument developed shall be referred to as a forward scattering photometer.

The particular problems associated with employing light scattering techniques to determine droplet size are best summarized by Sinclair (31) as follows

"(a) Each particle size makes its own contribution to the scattered light which cannot be distinguished from the others;

(b) These contributions are usually not unique since most light-scattering functions are multivalued; and

(c) Many observations do not distinguish between particle concentration and particle size."

To these three problems it is necessary to add a fourth, viz., for large particles that portion of the scattered light which is diffracted by the edge of the particle is contained within a very small solid angle forward of the particle. The problem is primarily one of distinguishing this diffracted light from the parallel transmitted beam.

The method of measurement of droplet size analyzed in this thesis is based on the decrease of intensity of a parallel light beam as it passes through an aerosol. If the equipment used to measure this decrease of intensity is properly arranged to exclude all of the scattered light, the measurement made will be that of the total scattering of all the particles of the aerosol included within the light beam. The basic equation which relates the transmission of light to the Mie theory is given in Appendix A. From

that equation, the following form of the transmission equation has been derived:

$$a_{\frac{3}{2}} = \frac{3}{4} \frac{w \; l \; K_{so}}{V \rho \; \ln \frac{E_0}{E}} \qquad (3)$$

where $a_{\frac{3}{2}}$ = volume-surface mean radius of the particles

w = weight of particles included in a volume V of the medium

ρ = density of the particles

$\frac{E_o}{E}$ = ratio of incident to emergent flux density of the transmitted beam

K_{so} = actual scattering area coefficient observed by the equipment

Two restrictions were applied in the derivation of equation (3), (a) the concentration must be small enough that the scattering is incoherent, and (b) each particle or droplet must have about the same value of K_{so}. The quantitative limit of concentration is unknown at present, particularly for large particles. The restriction that each particle have about the same value of K_{so} requires in effect, that each particle have about the same value of K_s, and, in addition, that the photometric equipment be so arranged that about the same percentage of the diffracted flux is excluded from the measurement of the emergent flux density of the transmitted beam.

The requirement that each particle have about the same K_s is easily satisfied for aerosols of large particles. The anticipated droplet distribution for air atomization is from 5 to

50 microns diameter. If blue light ($\lambda = 0.4$ microns) is used, the range of α equal to $\frac{2\pi a}{\lambda}$ is from 40 to 400. From the curve of K_s versus α for water droplets (Figure I), it is seen that K_s varies from 1.98 to 2.3, but the variation is much less over a major portion of the range. An average value for K_s from $\alpha = 40$ to $\alpha = 400$ is about 2.06. Therefore, for the case of water droplets atomized by a high velocity gas stream, the value of K_s may be assumed to be the same for each droplet, and equal to 2.0 or a few percent greater than 2.0.

The requirement that the photoelectric tube measuring intensity observe the same K_{so} for each particle requires an analysis of the angular distribution of scattered light and the optical system employed with the photometer. The light which is intercepted by the geometric cross section of a particle is scattered by reflection and refraction equally in all directions. It may therefore be assumed that practically all of this light is separated from the transmitted beam. The second component of the scattered light is that which is diffracted by the edge of the particle. For large particles practically all of this diffracted light is contained within a very small solid angle ahead of the particle, and is not separated from the transmitted beam until sufficient distance away from the aerosol. Previous investigators (3, 32) have observed this distance to be of the order of 18 feet for various optical systems with both uniform-sized particles (15 microns diameter) and non-uniform sized particles (25 and 34 micron volume-surface mean diameters).

A desire to effectively reduce this distance, and thus reduce the dimensions of the forward-scattering photometer, motivated the analytical studies of the diffraction pattern and optical system which are presented in this thesis.

The amount of diffracted light energy reaching the phototube depends upon two factors, (a) the solid angle originating from the particle included by the aperture, and (b) the amount of diffracted energy contained within this solid angle. An analysis has been made in Appendix C of the proposed optical system to determine the relationship between this solid angle, or "cone of observation", and the geometrical and optical constants of the system. The results of this snalysis show that the "cone of observation", represented by the plane angle ψ , is given by

$$\psi = \frac{r}{f} \tag{4}$$

where r = radius of the aperture in front of the photocell

f = focal length of the collecting lens.

Equation (4) showns it is possible to duplicate the long distance required to accomplish separation of the diffracted light by making the ratio of r/f as small as possible.

In order to predict the amount of diffracted energy which will be included within this "cone of observation", it is necessary to know the angular intensity distribution of the scattered light. The angular intensity distribution of the scattered light can be determined from the Mie theory. Angular distribution curves can be calculated using the intensity functions given in the tables

of "Light Scattering Functions for Spherical Particles". (6) Such curves have been calculated by Gumprecht, et al, (5) for a few values of α up to α equal to 40. At the higher values of α the calculations become more and more tedious as more terms are required for convergence. Since the distribution pattern would differ for each size particle, it would be necessary to calculate several such distribution curves to properly analyze the problem. Since time would not permit the calculations necessary to determine the angular distribution curves for several sizes of large particles, it was decided to make an approximate analysis such as suggested by Houghton (12). The approximate analysis consists of finding the angular distribution pattern of light diffracted by a small aperture, which is, according to Babinet's principle, the same as the distribution pattern of light diffracted by an opaque disc of the same radius. The equation giving the intensity of diffracted light, for a circular aperture, at any angle of observation is derived by Humphreys (13) and Johnson (16). The analysis is carried further in Appendix B of this thesis to determine the diffracted energy included within a solid angle originating at the particle. The results of this analysis are presented in Figure <u>II</u> which is a plot of the percent of diffracted energy excluded from a solid angle, represented by the plane angle θ, versus the parameter $\beta = \frac{\pi a \sin\theta}{\lambda}$, which represents the "cone of observation" for given particle size and wavelength.

The analysis of the optical system and the diffracted flux may be linked together to predict the value of K_{so} which a given

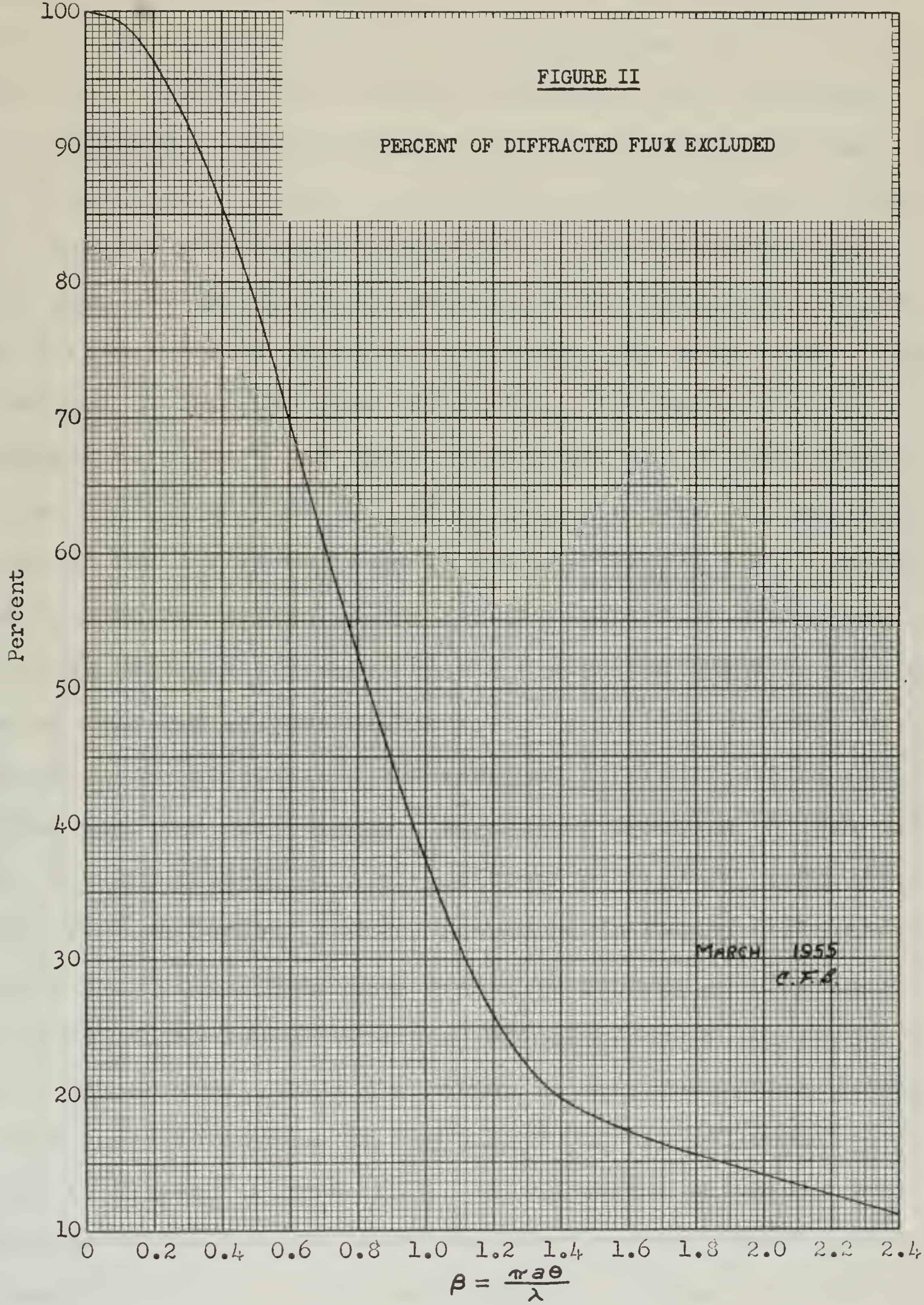

FIGURE II

PERCENT OF DIFFRACTED FLUX EXCLUDED

MARCH 1955
C.F.B.

photometer will observe. When the optical system is adjusted so that all of the diffracted light is excluded, the value of K_{so} will be about 2.0. (It has been assumed that all of the intercepted light is excluded.) If the optical system is arranged so that only 50% of the diffracted light is excluded, the value of K_{so} is about 1.5 (1.0 for the intercepted light plus .5 for diffracted light.) However, when the particles are not all of the same size, the percent of diffracted flux excluded will differ for each size. Since it is desired to have the same value of K_{so} for each particle it is necessary to make θ as small as possible and exclude nearly all of the diffracted flux ($K_{so} \cong 2.0$), or to make θ so large that none of the diffracted flux is excluded ($K_{so} \cong 1.0$). It was decided to base the design of the forward scattering photometer on the first of these choices, and the design was based on obtaining K_{so} as near 2.0 as practicable .

To check the adequacy of the combined diffraction flux-optical system analyses made herein, the data of Cheatham (3) was analyzed. His experiments on light scattering by glass beads were made with various lenses and various apertures in front of the photocell while varying distance from sample to photocell. The large number of variables thus provided an excellent means to compare predicted values of K_{so} with the actual values observed by Cheatham. This analysis is made in Appendix D and typical results are indicated in Figures IX and X . The agreement between predicted and observed values was considered good and sufficient confidence was gained in the approximate theory to proceed with the design of the experimental forward scattering photometer.

SECTION III

Description of Experimental Apparatus

The photometer described in this section serves a twofold purpose. First, the various components were assembled on an optical bench in the darkroom for calibration runs, using glass beads suspended in oil. This arrangement permitted a maximum amount of flexibility in the arrangement of the various lenses and apertures making up the optical system. The experience gained during the calibration runs and the interpretation of the results obtained has yielded sufficient information for the design of an actual laboratory instrument for droplet size measurement. This instrument employs many of the same components used for the static calibration runs. A schematic diagram of the calibration apparatus is contained in Figure III. The instrument designed for atomization studies is shown in Figures IV and V .

Calibration Apparatus

As indicated by the optical system analysis, the crucial parameter involved in the design is the ratio of aperture size to collecting lens focal length. A 50 cm focal length collecting lens was selected, as this would permit the use of a reasonable aperture size and still give filtering characteristics as good as those obtained by Cheatham and Sinclair in going to 18 foot distances. It was felt that a longer focal length lens would result in too bulky an instrument. To permit variation of the r/f ratio, various apertures were provided, ranging in size from .0200

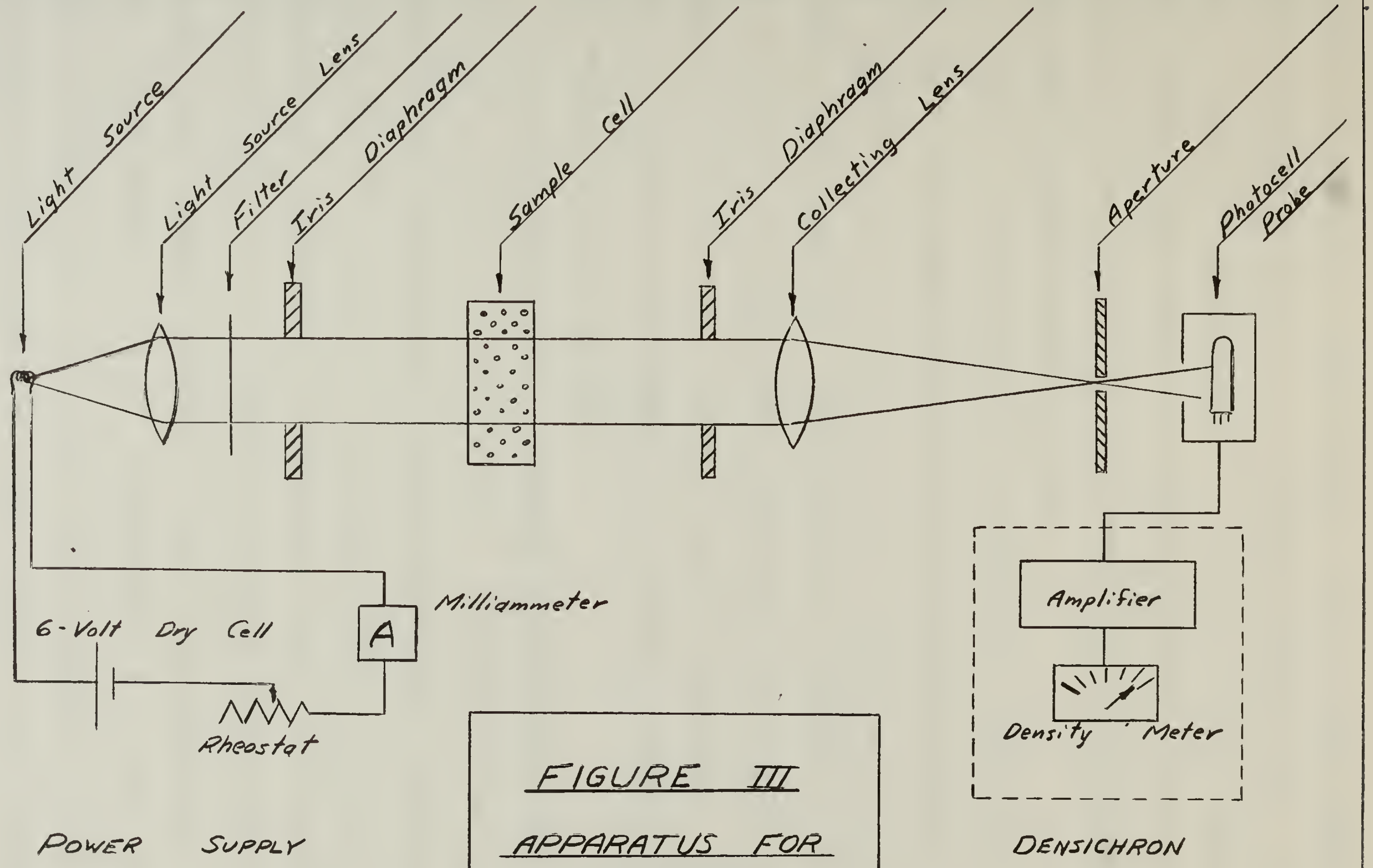

FIGURE III

APPARATUS FOR
STATIONARY
CALIBRATION

May 11, 1955

C.F.B.

inches in diameter to .422 inches. Six of these apertures were made by drilling holes in a 16 gauge aluminum plate, which was held in position approximately 6 inches from the photocell by a bench clamp. The remainder of the apertures could be attached directly to the face of the photocell probe, approximately 1/2 inch from the photosensitive unit.

When the r/f ratio is not controlling, the ratio of parallel light beam diameter to distance becomes important. To permit variation of this ratio, two iris diaphrams provided control of light beam diameter. For additional variation, the sample cell was located on a holder which could slide approximately 2 feet along the optical bench between the iris diaphrams. This holder contained guides so the sample cell could be exactly repositioned, once removed from the holder.

The light source was a standard hand lantern bulb, powered by a high capacity 6 volt dry cell. Control of the light source intensity was provided by a variable rheostat. It was found that by reducing the current to the light source to about 140 milliamps, satisfactory consistency of intensity could be obtained. A blue filter was placed in the system to provide monochromatic light. The spectral characteristics of this filter peaked at .410 microns, with a band width of .03 to .04 microns. A 6 inch focal length lens was located with the light source filament at its focal point to provide a nearly parallel light beam for the diffraction experiments.

The light intensity was measured by a commerical densitometer, the Densichron, manufactured by the W.M. Welch Manufacturing Co. This instrument consists of a photocell probe unit, an amplifier and a meter. The meter is a D'Arsonval type milliammeter with shaded pole pieces. The calibration is such that the scale reading equals the log of the reciprocal of the current, which in turn is directly proportional to the light intensity impinging on the photosensitive unit. This density reading will be referred to as D in this thesis. Thus, $D = \log_{10} 1/E$. The photocell employed in the probe has S-4 spectral characteristics, peaking at .400 microns wavelength. The sensitivity of the Densichron made it a highly satisfactory instrument for light intensity measurements. A linearity check, described in Appendix E, showed that this characteristic was excellent.

For the experimental runs comprising phase I, the photocell probe was mounted on an optical bench clamp, and was provided with a 1/2 inch aperture adjacent to the photosensitive unit. In phase II, this 1/2 inch aperture was replaced by the various apertures listed for each particular run.

The sample cell consisted of two plane glass faces, with sides of plexiglass. The inner distance between the glass faces, and therefore the light path length in the aerosol, was measured with a standard inside micrometer and found to be .995 inches.

The entire system, from light source to photocell probe, was mounted on a double rod optical bench. This permitted the desired flexibility in variation of the experimental parameters.

Alignment consisted of :

(1) Adjusting the light source lens so that a parallel beam of light was attained.

(2) Adjusting the filter, diaphrams, and collecting lens so that they were centered in this parallel beam.

(3) Locating the aperture so that it was centered at the focal point of the collecting lens.

(4) Adjusting the photocell probe so that the diverging light rays passing through the aperture were just captured by the 1/2 inch aperture on the probe. In phase II, this was not necessary, as the aperture was located directly on the probe.

For phase II of the experimental program, the smaller apertures were directly attached to screw fittings, which could be attached to the photocell housing. A piece of frosted plastic was placed just inside the housing, between the aperture and the photosensitive unit,to disperse the concentrated light rays over the element. It was felt that this precaution would avoid supersaturating any one point on the cathode of the photoelectric cell.

Atomization Photometer

The instrument to be used in atomization studies is shown schematically in Figure IV. Figure V is a photograph of the instrument with the sides of the light tight casing open to show the components. The overall length of the photometer is approximately five feet.

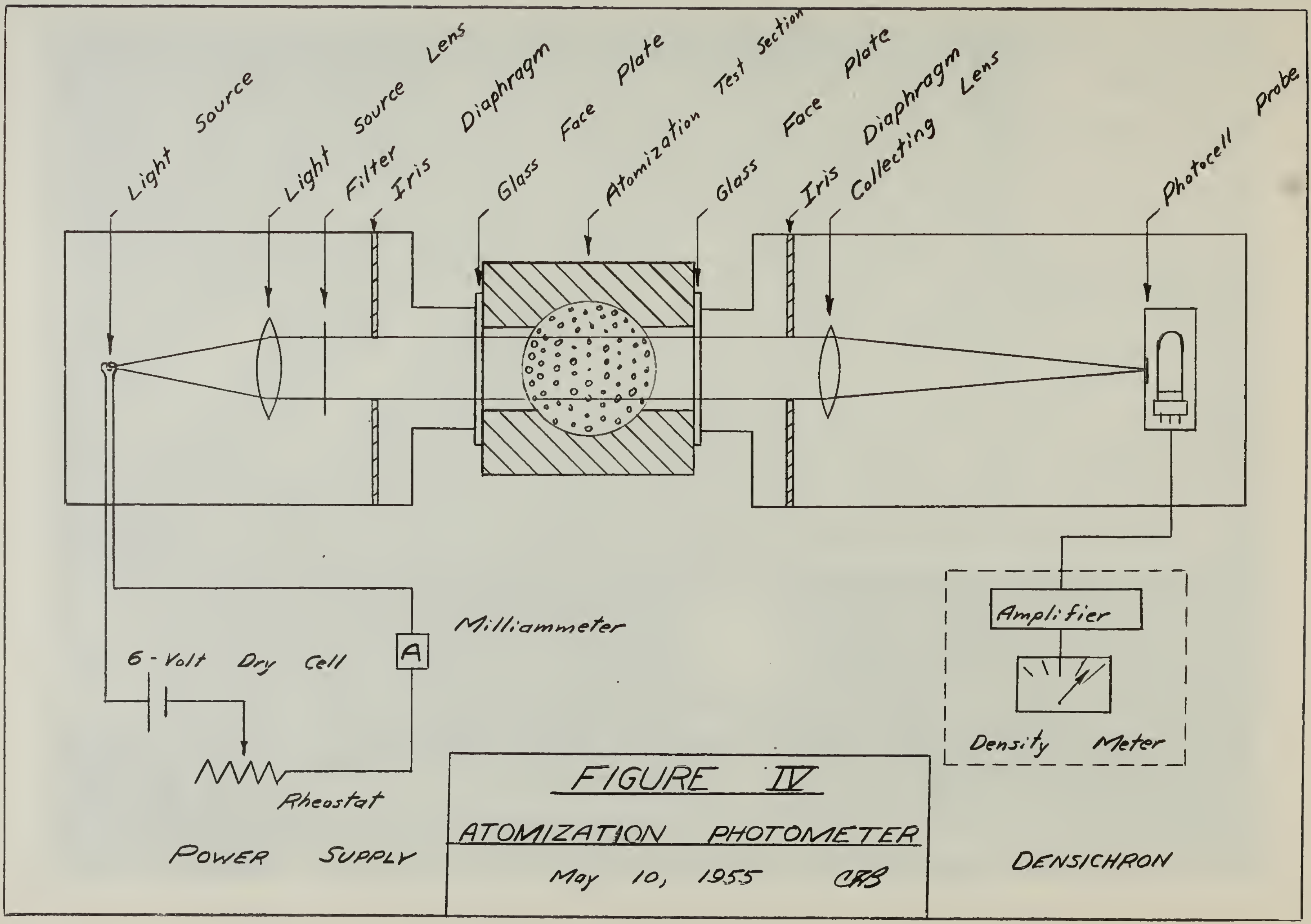

FIGURE IV

ATOMIZATION PHOTOMETER

May 10, 1955 CRB

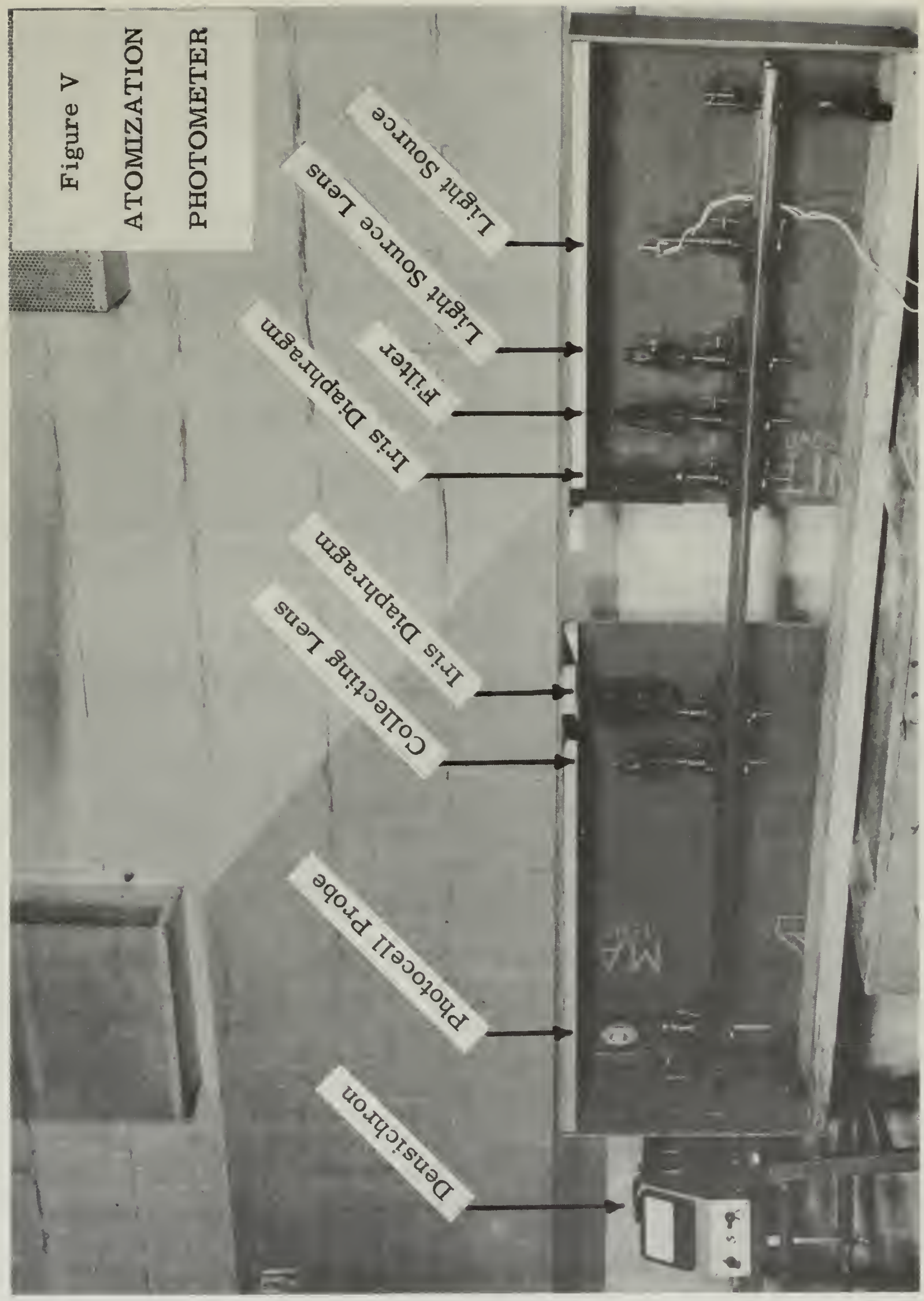

Figure V
ATOMIZATION
PHOTOMETER

As a result of the experience gained during the stationary calibration runs, it was decided to incorporate the 50 cm focal length collecting lens and the .0625 inch diameter aperture in the final atomization photometer. This aperture is attached directly to the photocell probe face. A piece of frosted plastic is located between the aperture and the photocell itself. For a full discussion of the factors underlying this choice of components, see Section VI, Discussion of Results. The other components, such as the light source, filter, light source lens, iris diaphrams, power supply, and Densichron, used in the stationary calibration apparatus are incorporated unchanged in the atomization photometer.

Due to the sensitivity of the Densichron, and in order to preclude extraneous results due to light from the room, the entire optical system is enclosed in a light tight casing. This casing can be attached directly to the test section and sealed, thereby excluding all room light. The interior of the casing is painted a dull black to eliminate secondary reflection of the scattered light. The power supply and Densichron are separate units.

SECTION IV

Experimental Procedure

General

The majority of the experimental work involved in this thesis was aimed towards verifying the approximate theories advanced as a basis for a rational design of a photometer. By working with glass bead, whose size could be determined by other procedures, an experimentally observed scattering area coefficient, K_{so}, could be compared with the predicted value. The various significant parameters were systematically varied to determine their effect. Initial calibration runs were made with the beads suspended in oil. A final series of runs was made on a dynamic calibration apparatus, in which the beads were carried past the photometer by a high velocity air stream. This apparatus closely approximates the conditions under which droplet sizes will be measured in an air atomization study.

Stationary Calibration

A description of the experimental apparatus is given in Section III. Two different sizes of glass beads were used for the calibration runs, 26.6 and 30.1 microns volume-surface mean diameters. A description of these beads and the method of size determination is given in Appendix F. The glass beads were suspended in Dow-Corning 550 silicone oil for the diffraction measurements. Due to the sensitivity of the Densichron, all of the

stationary calibration runs were carried out in a darkroom.

The experimental apparatus permitted the variation of the following parameters:

(1) Aperture size, 2r
(2) Iris diaphram setting, 2R
(3) Collecting lens focal length, f
(4) Distance of sample cell from the collecting lens, f + c
(5) Concentration of beads in the mixture
(6) Size of the beads

The analysis of the optical system permitted the reduction of these 6 variables to the following four:

(1) Ratio of aperture size to lens focal length, r/f
(2) Ratio of iris diaphram setting to distance, R/f + c
(3) Concentration of beads
(4) Size of beads

The bead size was chosen with the estimated size of the droplets to be investigated in atomization studies in mind. Calculations of the predicted actual K_s from the Mie theory approximation, as outlined in Appendix B, show that for both of the bead sizes considered, K_s should be within 3% of a value of 2.0.

The analysis of the optical system contained in Appendix C indicated that it would be desirable to use a small ratio of aperture size to focal length so that the observed value of K_{so} could approach 2 as closely as possible. However, the gain to be realized by using expremely small apertures rapidly diminishes.

For example, the predicted K_{so} values for the 26.6 micron beads and a 50 cm focal length collecting lens for various aperture sizes is as follows:

Aperture Diameter	K_{so}
.105	1.94
.0625	1.975
.0400	1.99

The experimental program was divided into two major parts. In the first phase, the distance from the aperture to the photocell was of the order of 6 inches. Distance, r/f, bead size and concentration were varied. Analysis of the data for this phase indicated that, although consistent results had been obtained, there existed a systematic deviation of K_{so} from that predicted by theory. It was believed that diffraction effects around the aperture itself were responsible for the poor agreement with the approximate theory. For a complete discussion of these results, see Section V.

In order to eliminate the aperture diffraction effects, the aperture was placed on the face of the photosensitive unit, and the general procedure of phase I repeated. This series of experimental runs will be identified as phase II.

The actual experimental procedure can be best illustrated by the description of a typical experimental run. The optical system was first aligned so that the light source image was either centered on the aperture, or swallowed by it as the case may be. A zero reading was then taken, designated by D_{oo}, in which the sample cell was not in place. The purpose of this

reading is merely to properly zero both the light source intensity and Densichron volume control. Next, the sample cell faces were carefully cleaned and the sample cell filled with clean oil. D_o readings were then taken at various distances, care being taken that the sample cell was positioned exactly against the guides on the holder. These D_o readings were taken at least 2 or 3 times to insure that the positioning of the sample cell could be duplicated. The iris diaphram opening was then adjusted to a new position and new D_{oo} and D_o readings were taken.

Once consistent D_o readings had been obtained, the oil was emptied from the sample cell into a graduate. This graduate was then weighed and the oil poured into a flask. The empty graduate was then weighed and the weight of oil computed. Next, the weight of beads was determined using a chemical balance. The beads were poured into the oil and the mixture stirred carefully for 15 to 20 minutes. It was found that extreme care must be exercised while stirring in order to prevent air bubbles becoming entrapped in the mixture, and at the same time to produce a uniform distribution of the beads in the mixture.

The mixture was poured into the sample cell and the few air bubbles which inevitabily became entrapped during the pouring were allowed to rise. This took from 5 to 10 minutes. Since some of the beads had also settled during this time, it was then necessary to stir the mixture gently to redistribute the beads. The final portion of this mixing period was carried

out with sample cell in position on the optical bench with density readings being taken at regular intervals of time. At first the density readings would consistently increase, as beads were being stirred up from the bottom of the sample cell. However, these readings leveled off after a short time. This was taken as an indication that the beads were uniformly mixed in the solution.

The final step involved taking the D readings at the same iris diaphram and distance settings as before. Before taking these D readings, the Densichron and light source were adjusted to reproduce the D_{oo} or zero readings obtained at first.

In general this experimenal procedure requires considerable patience and care to obtain reproducible results. The stirring of the mixture must be slow and gentle so as not to introduce air into the solution. This stirring must be carried out intermittantly between each D reading to prevent settling of the beads. Constant checks of the D_{oo} reading must be made to insure that the light intensity or Densichron response has not changed. These fluctuations were found to be small, but sufficient to introudce errors of the order of 5 or 10% if not watched. Since it is necessary to remove the sample cell from the holder to obtain a D_{oo} reading, care must be taken to reposition it in exactly the same manner as before. One final point to be observed is that the faces of the sample cell must under no conditions be touched or cleaned between the D_o and D readings.

In phase I there was no means of positively repositioning the aperture, so only one aperture setting could be used for each separate weighing of the beads. The only variables available in a single run were the iris diaphram setting and the distance, which combine to form the $R/f + c$ ratio. In phase II, however, the apertures could be screwed into the face of the photocell unit, and thus their previous position could be reproduced if they were removed. Therefore, aperture size, as well as the $R/f + c$ ratio could be varied for each weighing. With this exception, the experimental procedure for phase II was exactly the same as that for phase I.

Dynamic Calibration

Having verified the approximate theory and the reliability of the photometer in phases I and II of the stationary calibration, the next step was to attempt size measurements of glass beads under conditions which closely approximate those under which air atomization studies will be made. For this purpose an experimental apparatus in which glass beads can be injected into a high velocity air stream was used. This apparatus is fully described by Gottling(39).

Since the geometry of the photometer had been fixed, the only variables available in these experimental runs were the mass rates of flow of air and beads. From the photometer point of view these two flow rates reduce to one variable , viz. that of particle concentration. However, it must be realized that flow conditions in the test section are dependent on each of

these two variables.

The air flow rate could be adjusted to the desired value by controlling the back pressure to the test section. Before starting the bead feeder, a D_o reading was taken on the Densichron. The bead feeder was then turned on, flow rate control being provided through the variable speed DC motor drive. Once steady state conditions had been reached, which normally occurred after 10 or 15 seconds, optical density readings and test section static pressure readings were taken. The cylinder containing the beads was weighed before and after each run and the exact length of time of each run measured. With these readings, the mean bead flow rate could be easily determined.

Once a run had been completed a check was made on the zero reading of the Densichron. In most cases a slight increase in optical density was recorded, the cause of which can be attributed to a few beads adhering to the glass face plates. However, this effect was considered negligible.

The fluctuations in the bead flow rate were readily discernible on the Densichron meter. The recorded meter readings were actually a mean of these fluctuations, which amounted to 20 or 30% of the mean reading in extreme cases. It was noted that the optical density readings, and presumably the bead flow rate, tended to be consistently higher at the beginning of the run than at the end.

SECTION V

Discussion of Results

The goal of the experimental program was to investigate and substantiate the analyses proposed herein as the basis for the design of a forward scattering photometer. The major portion of the experimental data was taken under carefully controlled conditions with glass beads suspended in oil. Additional data was taken on a test set-up in which glass beads were carried past the photometer by a moving air stream. As far as possible, the significant parameters which entered into the analysis were varied separately in order to determine their individual effects and the limitations of the analysis. The results may be conveniently divided into three separate groupings: (1) stationary calibration, phase I; (2) stationary calibration, phase II; and (3) dynamic calibration. Original data is contained in Appendix H, with sample calculations being presented in Appendix I.

Stationary Calibration, Phase I

The distinguishing feature of this phase of the experiment was the separation of the aperture from the photocell by a distance of about six inches. The actual distances were determined experimentally to allow the cone of light from the aperture to just fill the large opening of the photocell housing. The results obtained are plotted in Figure VI as values of K_{so} versus the non-dimensional distance parameter $\frac{f+c}{R}$.

The geometrical and optical arrangement for this phase was

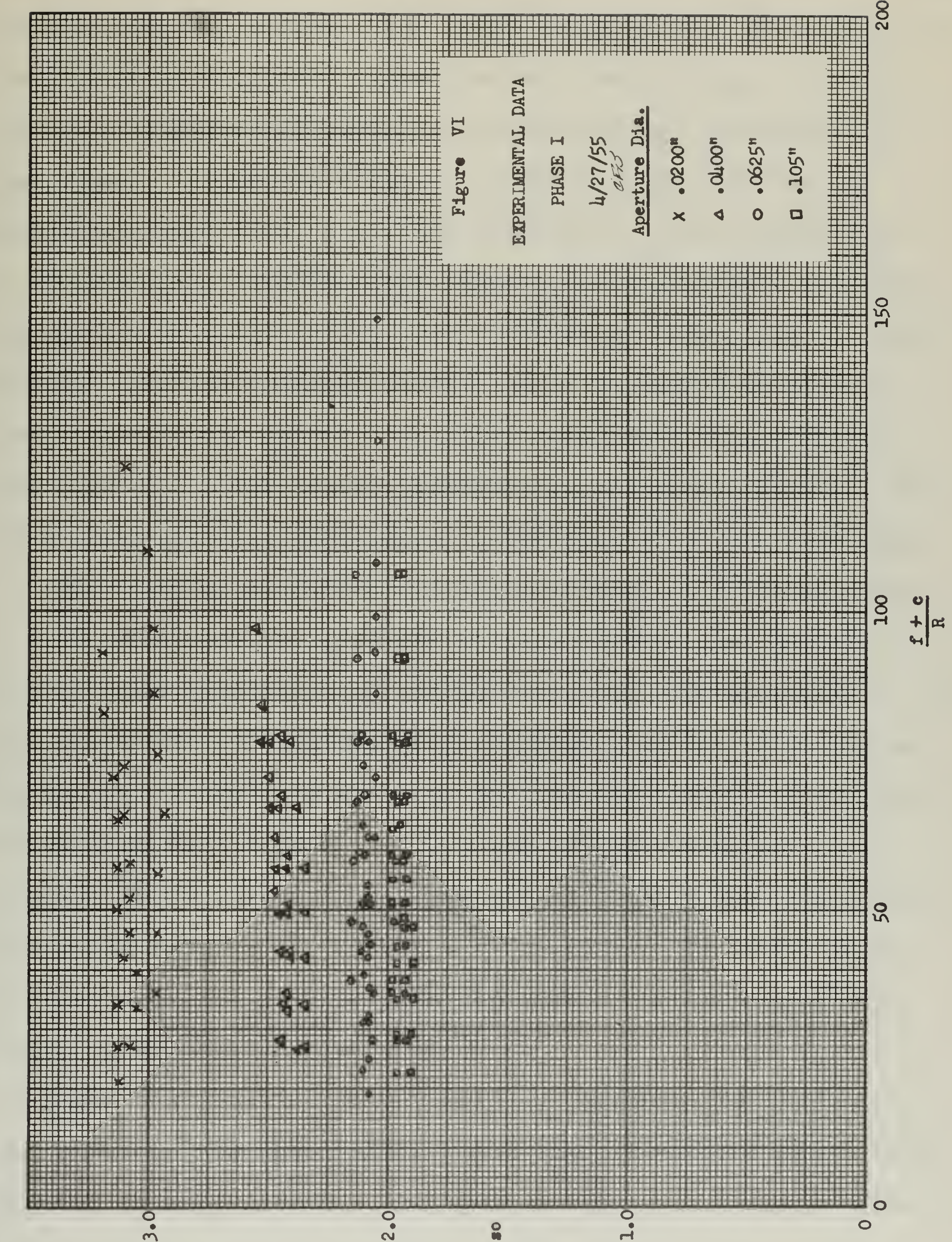
Figure VI
EXPERIMENTAL DATA
PHASE I
4/27/55
Aperture Dia.
x .0200"
△ .0400"
○ .0625"
□ .105"
K_so
3.0
2.0
1.0
0
0
50
100
150
200
f + c / R

selected for two reasons: (1) practically all of the diffracted flux would be excluded, therefore the predicted K_{so} was nearly 2.0 and (2) the aperture would be controlling throughout the test range. Figure VI clearly illustrates that the second prediction held true, i.e., the observed K_{so} was independent of the distance from the test cell to the photocell. However, the predicted values of K_{so} for the various apertures differed greatly from the observed values. For the smallest aperture used, .0200", the observed K_{so} was about 50% higher than the predicted K_{so}. The larger apertures gave similar results, the error progressively decreasing as aperture size was increased.

The results presented for any aperture size include two or more runs made at different concentrations. No apparent effect of bead concentration can be observed, any variation in the data appearing to be normal experimental scatter. The reproducibility of the data for a given geometry using various concentrations (cf. runs 8, 11, 13, and 14) is considered to be adequate proof that mutual interference between beads does not affect the results for concentrations within the range of investigation. The maximum concentration used had a bead separation to diameter ratio of about 8.

Since bead concentration could not account for the consistent error in the observed K_{so}, and since the error was related directly to aperture size, it appears that a secondary diffraction occurs around the aperture itself. The window in the photocell probe was a 1/2 inch circle. Thus, a secondary "cone

of observation" is introduced, with an angle defined by the 1/2 inch window and the distance from aperture to photocell of 6 inches. This angle is fairly large when considering diffraction patterns for parallel light, but it must be remembered that the light incident on the aperture is not parallel. This type of diffraction by a circular aperture of light of varying direction is highly complex and not capable of simple analysis. Therefore, these effects may be treated only in a qualitative manner.

If secondary diffraction effects were the real cause of the unpredicted results, the effect should be eliminated by placing the aperture on the face of the photocell probe. With this location, the light rays deflected by secondary diffraction would still impinge on the cathode of the photocell, due to the large angle it subtended from the aperture. In so doing, however, a relatively intense point of light would be directed on the cathode. In order to circumvent the possibility of saturation of the photocell by this point of light, a piece of frosted plastic was placed behind the aperture to disperse the incoming rays, thus providing more uniform illumination of the cathode.

Summarizing, the important results of phase I were:

(1) The optical and geometrical arrangement employed eliminated the distance from the test cell to the photocell as a variable. The aperture was found to be controlling, as predicted.

(2) Results appeared to be independent of concentration. This is of importance for atomization studies, since the extreme condition anticipated is with a mass flow ratio of water to air of about 0.3. This corresponds to a droplet spacing of about 11 diameters for 20 micron droplets. This separation is greater than the minimum spacings used in phase I.

(3) Diffraction by the aperture itself must be considered in the design of a photometer. This result led to the investigations made in phase II.

Stationary Calibration, Phase II

Since it had been established in phase I that the distance effects had been removed from the instrument, the effort in this phase was concentrated on the effect of aperture size. Accordingly, the experimental data is plotted in Figure VII as K_{so} versus aperture diameter. Also included on the plot is the curve of K_{so} which the approximate theory predicts.

It is highly gratifying to see the correlation of the data with the theory. Due to the many assumptions entering into this theory, such excellent agreement was not expected. However, for the 38 data points taken in this phase, agreement to within a maximum error of 5% has been obtained. A 5% scatter of measured values is considered to be entirely within the limits of experimental accuracy.

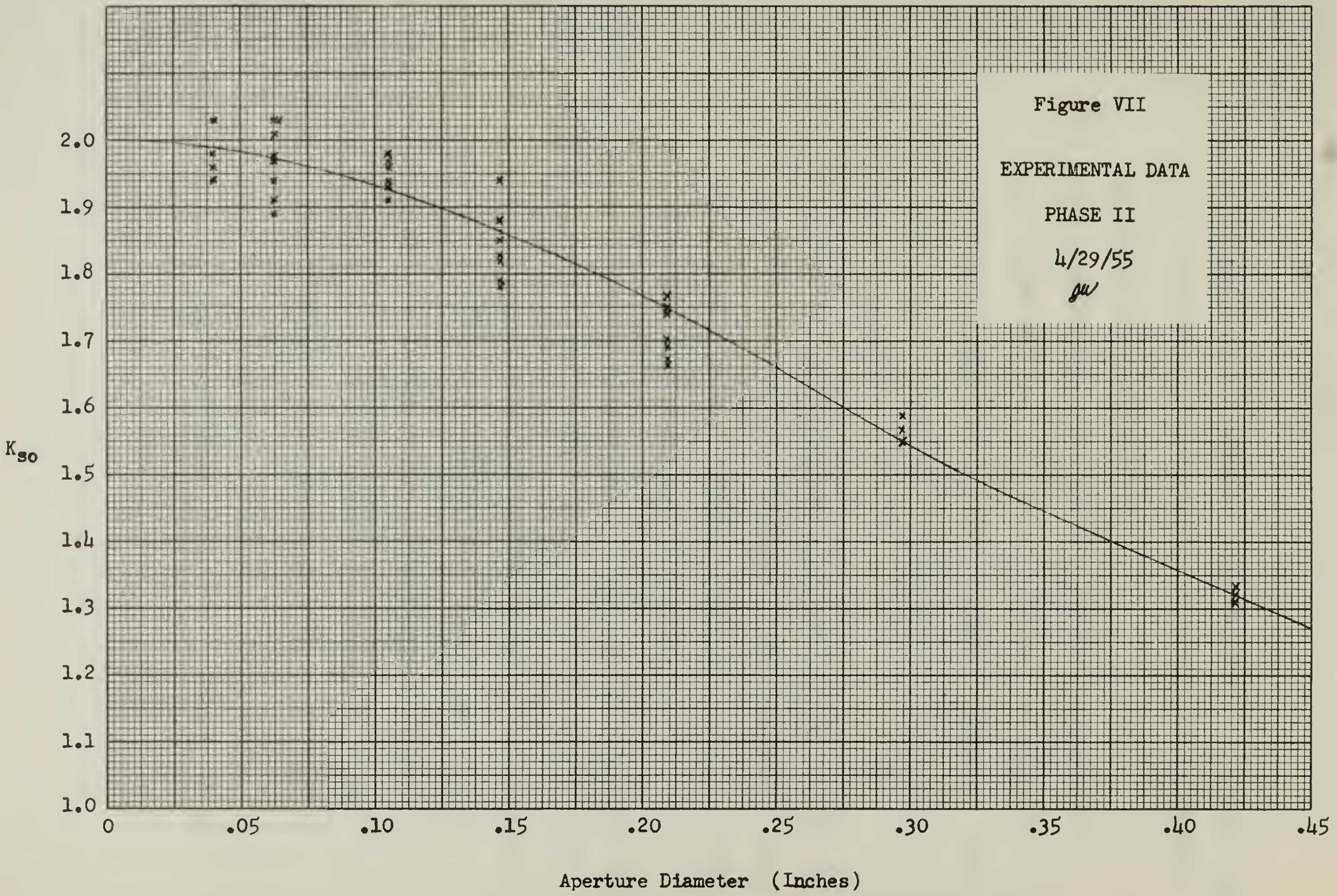

Figure VII

EXPERIMENTAL DATA

PHASE II

4/29/55

As a consequence of the results obtained in phase II, it may be concluded:

(1) The approximate theory is capable of predicting the performance of a forward scattering photometer quite closely.

(2) The secondary diffraction effects around the aperture may be circumvented by placing the aperture adjacent to the photocell probe, provided steps are taken to prevent saturation of the cathode.

(3) The forward scattering photometer with a 50 cm focal length collecting lens and either a .0625 or a .0400 inch diameter aperture will be satisfactory for atomization studies.

Although slightly more effective filtering will be obtained with an aperture smaller than .0400 inches, the absolute intensity of the light captured drops rather rapidly. This is primarily due to the fact that, for apertures less than .0625, the light source image is larger than the aperture hole. It is considered desirable for the aperture to capture as much of the light source image as possible and still give predicted values of K_{so} within 2 or 3 percent of 2.0. Therefore, a .0625 inch aperture was selected for use in the final phase of the test program.

Dynamic Calibration

The geometry of the photometer was held constant in this phase, since it had been determined in phase II that the system selected would be capable of measuring K_{so} to within 3%. Taking $K_{so} = 1.975$, particle sizes may be computed from the observed data, in the manner outlined in Appendix I, Sample Calculations. The results are summarized in Table 1, below, the original data being presented in Appendix H.

TABLE 1

Bead Diameters as Measured by Photometer

Run No.	w_b/w_a	M_1	d(microns)
1	.229	.285	22.1
2	.229	.285	21.5
3	.183	.374	17.1
4	.175	.374	21.3
5	.140	.456	21.1
6	.144	.454	20.5

Note: M_1 is the Mach No. at the nozzle throat.

With the exception of run #3 the particle sizes are consistent to within 7%, the tendency being for the measured diameter to decrease with increasing air flow rates. It is believed that the erroneous results for run #3 are due to an error in reading the static pressure manometers.

The actual size of the glass beads used for calibration was measured by Gottling using a differential settling technique to be 25.8 microns. An independent size measurement of the beads before use in the dynamic calibration apparatus is

[illegible]

[illegible]

[illegible]

[illegible]

[illegible]	[illegible]	[illegible]	[illegible]
[illegible]	[illegible]	[illegible]	[illegible]

[illegible]

[illegible]

described in Appendix F of this thesis, giving the diameter as 26.6 microns. It is fairly well established that the bead diameter is in the neighborhood of 26 to 27 microns. Based on this information, the photometric measurement appears to have an error of approximately 25%.

The following possible causes of this error have been considered, and will be discussed briefly:

(1) Air flow rate measurements

(2) Effective path length in the medium

(3) Fluctuations in the bead flow rate

(4) Bead and velocity profiles in the test section

(5) Foreign particles, such as dust

(6) Instrument errors in the photometer

Air flow rate determination was based on the assumption of isentropic, one dimensional flow in the nozzle. Past experience has proven that this assumption is a fairly good one, nozzle correction coefficients being of the order of 96% to 98%. In the present set-up the tube through which the beads were injected extends along the centerline of the nozzle and will introduce additional frictional losses. However, the magnitude of these losses should be only a few percent at the most.

The actual area upon which the air flow rate was based was taken as that of the full test section, disregarding the loss in area caused by the bead injection tube. As the outside diameter of this tube was only .377 inches, compared to the test section I.D. of 2.0 inches, it can be easily determined that

this correction would amount to less than 4%. The validity of making such a correction is open to question, however, as there is some air flow through this tube.

Both of the two possible errors in air flow rate tend to reduce this quantity. This, in turn, will cause the actual velocity of the particles at the photometer to be smaller than calculated. Reference to the transmission equation (G-3) shows that if the actual velocity was smaller, the measured particle size would be larger. Thus corrections for such effects would tend to reduce the observed error in particle size.

The light path length used for calculation purposes was 2 inches, the inside diameter of the test section. Actually, the distance between the glass plates covering the test section was 3 inches (see Figure IV). In the event that eddies were formed in the spaces between the glass plates and the test section, the effective path length would be greater than 2 inches. Moreover, the concentration of the beads in these spaces would differ greatly from the concentration in the air stream. It is not possible to analyze this error quantitatively; however, any increase in the effective path length of the light beam reduces the observed error. It is recommended that special ports be made for the equipment which will limit the path length to the inside diameter of the test section and thus preclude the possibility of eddy formation.

Fluctuations in the bead flow rate were of two distinct

and separate types. First, the bead flow rate, as inferred from the Densichron readings, was somewhat higher during the initial portion of any one run, settling down after about 10 or 15 seconds. Second, rapid fluctuations about a mean were observed throughout the run. The effect of the second class of fluctuations is difficult to assess. However, the consistency of the readings for different runs indicates that any errors due to the continual fluctuations are small.

The first type of variation may have a significant effect. The static pressure manometer readings were generally taken early in the run, there being insufficient time for a complete set of readings near the end. If the instantaneous bead rate of flow is larger than the mean, the drag forces will cause a larger pressure drop between the throat of the test section nozzle and the static pressure tap at the photometer. This erroneous pressure reading will cause a higher velocity V_2 to be inferred than actually exists. Such an error will again cause the measured diameters to be smaller than the actual sizes.

In the calculations of bead sizes from photometric measurements it was implicitly assumed that the distribution of particles was uniform throughout the aerosol. However, such is not the case when the beads are entrained in a high velocity air stream. The local bead rate of flow per unit area, w_b/A, will vary across the diameter, as will bead velocity. To investigate these effects it is necessary to write the transmission equation in the form

$$\ln \frac{E_o}{E} = \int_0^l S\, n\, dx$$

where n is now a function of x, and not a constant, as assumed before.

The expression for n given in Appendix G is,

$$n = \frac{w_b \times 6}{A V \pi d^3 \rho_b}$$

It can be seen that it is necessary to know both w_b/A and V as a function of the distance across the test section, x. The velocity profile can be determined from a stagnation pressure traverse. However, this information is unavailable at present. Gottling has obtained experimental profiles of w_b/A. A representative sample of these profiles shows the curve of $\frac{w_b/A}{(w_b/A)_{avg}}$ to peak at the centerline at about 1.12, with a fair approximation of the shape being obtained with a straight line intersecting the wall at a value of .94. Integration of this straight line will yield a value of the total bead rate of flow equal to $(w_b/A)_{avg}$ times the total cross-sectional area. Calculations of ln E_o/E using this straight line profile show that this effect will raise the measured diameter by 3%.

By referring to the expression for n, it is apparent that if the velocity profile and the w_b/A profile were both taken into account, the effects would tend to cancel one another. w_b/A and velocity should both tend to be smallest at the wall

$$[illegible]$$

[illegible]

$$[illegible]$$

[illegible]

[illegible]

and largest at the test section centerline. It is not inconceivable that such variations may well cancel, leaving n essentially constant along the light path length.

Small particles of dust may be drawn into the test section from the room or become mixed with the beads after continued usage. In addition, lint from the bead filter bags will be introduced. This effect, while difficult to evaluate is felt to be small.

Finally, the photometer itself should be considered as a possible source of error. The data taken in phase II of the stationary calibration proved to be quite consistent and reproducible. It is to be noted that exactly the same optical system used in the dynamic calibration was also used for a considerable amount of the experimental work in phase II. Therefore, it is the authors' opinion that the source of the 25% error lies not in the photometer, but rather in the measurements associated with the dynamic calibration apparatus.

In summary, the dynamic calibration runs yielded a volume-surface mean diameter for the glass beads which was approximately 25% too small. The results, however, were consistent, with the error increasing slightly for lower concentrations. Several possible sources of error have been considered qualitatively and it appears that each of these possible errors tends to yield a mean diameter which is too small. It therefore appears that further experimental and analytical work is required

so that these errors may be accounted for and eliminated if possible. It is believed that once the various effects have been properly investigated and evaluated that the photometer developed will be capable of providing a measure of the volume-surface mean diameter which is accurate to within a few percent.

SECTION VI

Conclusions and Recommendations

Conclusions

The Mie theory of light scattering by spherical particles shows that the scattering area coefficient, K_s, approaches a value of about 2.0 when the particle diameter is large compared with the wave length of the incident light. In order that a given optical system will actually observe this value of 2.0, it is necessary that all of the diffracted light be excluded from the photometric measuring device. An approximate analysis has been developed which permits a prediction of the percentage of diffracted light which can be excluded from a photocell for a given optical system. A photometer was designed and calibrated based on this analysis.

From the results of this calibration it is concluded that:

(1) the analysis developed can be used to rationally design a photometer and to predict its accuracy within a few percent;

(2) the photometer will permit the measurement of the volume-surface mean diameter of particles in an aerosol when the concentration of the particles is known;

[illegible]

[illegible]

[illegible]

[illegible]

[illegible]

(3) the photometer developed does not depend on distance to separate the diffracted light from the transmitted parallel light;

(4) care must be exercised in the selection and placement of the aperture used in front of the photocell so that diffraction by the aperture itself is not encountered;

(5) mutual interference of the diffracted light between droplets will not be of any significance in atomization studies; and

(6) the dynamic calibration data, alghough erroneous, indicates it is possible to apply the photometer directly to the measurement of droplet size in a high speed air stream.

Recommendations

It is felt that the correlation of the results of the Stationary Calibration, Phase II, with the predictions indicate that no further investigations of a stationary nature are required. It is recommended, however, that the dynamic calibration testing be continued to determine the magnitudes of the various errors enumerated in the Discussion of Results. It is the authors' opinion that these errors can be accounted for. In connection with the continuance of the dynamic calibration, it is specifically recommended that:

(1) test section ports be altered to provide a path length

equal to the inside diameter of the test section;

(2) air filters be provided on the air intake to reduce the amount of dust mixing with the glass beads;

(3) replace the beads currently in use with clean beads;

(4) determine the properties of the new beads used, i.e. the density and volume-surface mean diameter;

(5) alter experimental technique by using longer times for the runs to permit determination of better average values; and

(6) calibrate the nozzle used so that the air mass flow rate may be determined more accurately.

Once the above recommendations have been followed and the dynamic calibration obtained to within a sufficient degree of accuracy, the photometer described in this thesis should be capable of providing a reliable measure of droplet size in atomization studies. The equations developed in Appendix G permit a convenient tabular form to be employed in the calculations.

SECTION VII

APPENDIX

APPENDIX A

The Transmission Equation

For an aerosol of transparent particles of uniform size, the transmission of a parallel beam of light through the aerosol has been found experimentally to be (see Sinclair (30) and Handbook on Aerosols (7)).

$$\frac{E}{E_o} = e^{-Snl} \qquad \text{(A-1)}$$

where E_o = flux density of the incident parallel beam

E = flux density of the parallel beam after passing a distance l through the aerosol

n = number of spheres of radius a per unit volume of the medium

S = scattering cross section

This equation holds for light of a single wave length and for aerosols where the individual particles are far enough apart so that the scattering is incoherent.

When the aerosol is composed of non-uniform size particles, the product nS is given by

$$nS = \sum_{o}^{n} K_s \pi a^2 \qquad \text{(A-2)}$$

where the summation is performed over all sizes of particles using the appropriate value of K_s for each size. Combining this expression with equation (A-1) gives

$$\frac{E}{E_o} = e^{-l \sum_{0}^{n} K_s \pi a^2}$$

$$\text{or } \ln \frac{E_o}{E} = l \sum_{0}^{n} K_s \pi a^2 \qquad \text{(A-3)}$$

The total weight of the particles, w, present in an aerosol of volume V is given by

$$w = V \sum_{0}^{n} \frac{4}{3} \pi a^3 \rho \qquad \text{(A-4)}$$

where ρ = density of the particles

To convert equation (A-3) to a useful form, multiply the right hand side by w and divide the right hand side by the equivalent of w given in (A-4) to obtain

$$\ln \frac{E}{E_o} = l \sum_{0}^{n} K_s \pi a^2 \left[\frac{w}{V \sum_{0}^{n} \frac{4}{3} \pi a^3 \rho} \right]$$

Rearranging this result gives

$$\frac{\sum_{0}^{n} a^3}{\sum_{0}^{n} K_s \; a^2} = \frac{3wl}{4 \rho V \ln \frac{E_o}{E}} \qquad \text{(A-5)}$$

All quantities on the right hand side of equation (A-5) can be determined for any particular experiment employing the forward scattering method. It is therefore possible to obtain experimental values for the quantity

$$\frac{\sum_{0}^{n} a^3}{\sum_{0}^{n} K_s \, a^2}$$

In those cases where the value of K_s is the same for each particle of the aerosol and this value of K_s is known, it is possible to obtain experimental values for the quantity

$$\frac{\sum_{0}^{n} a^3}{\sum_{0}^{n} a^2}$$

which is, by definition, the volume-surface mean radius of the particle spectrum. Since K_s cannot be exactly the same for each particle unless they are all the same size, and since the actual K_s cannot be observed exactly with forward scattering techniques, the transmission equation for an aerosol of particles of non-uniform size becomes

$$a_{\frac{3}{2}} \equiv \frac{\sum a^3}{\sum a^2} \cong \frac{3}{4} \quad \frac{wl \quad K_{so}}{\rho V \ln \frac{E_o}{E}} \qquad (3)$$

where K_{so} is used in place of the actual K_s to permit a correction for the diffracted light which is captured by the photosensitive unit.

Equation (3) is the working equation for obtaining the approximate volume-surface mean radius using a forward scattering photometer. See Section II for more details on the application of equation (3) to experimental work.

APPENDIX B

Analysis of Scattered Flux Distribution

The analysis of the angular intensity of light diffracted by an opaque sphere is given by Humphreys (13) and Johnson (16). The results are applied here to derive an approximate method by which the diffracted light energy contained within a small solid angle ahead of the sphere may be calculated. See Section II, Theoretical Considerations for Design of a Photometer, and Appendix D for further details on application of this analysis.

Consider a droplet of radius "a" illuminated by plane parallel radiation. The intensity of the diffracted light at any angle θ (measured from the direction of the incident light) is given by Johnson (16) in the form

$$I_D = \pi^2 a^4 \left[\frac{1}{\beta} J_1 (2\beta) \right]^2 \qquad \text{(B-1)}$$

where: a = radius of the particle

$\beta = \frac{\alpha}{2} \sin\theta$

J_1 = Bessel function of the first order

$\alpha = \frac{2\pi a}{\lambda}$

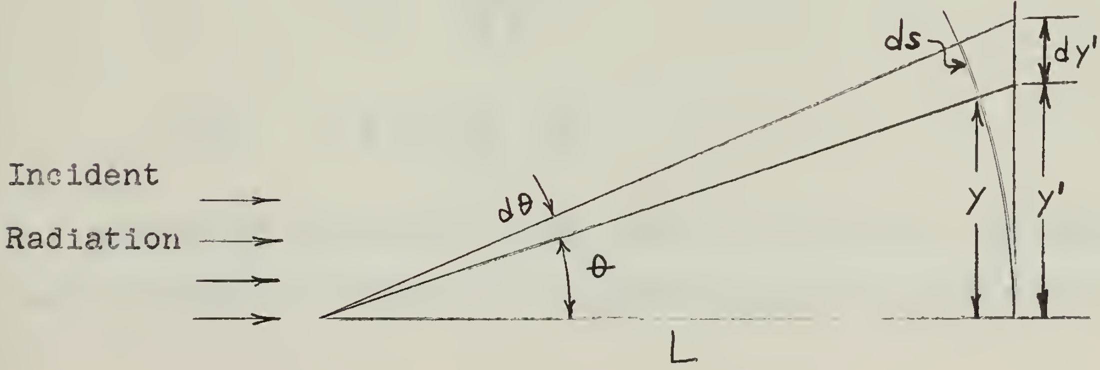

[illegible]

[illegible]

[illegible]

$$[illegible]$$

[illegible]

$$[illegible]$$

[illegible]

$$[illegible]$$

[illegible]

The diffracted flux passing through the incremental area $2\pi y'\,dy'$ shown in the sketch is given by the relation

$$dF = I_D \times dw = I_D \times \frac{d(\text{Projected Area})}{L^2}$$

$$d\,(\text{Projected Area}) = 2\pi y\,ds = 2\pi yL\,d\theta$$

$$d\,(\text{Projected Area}) = 2\pi L^2 \sin\theta\, d\theta$$

hence: $dF = 2\pi I_D \sin\theta\, d\theta$

The diffracted flux contained within the angle θ is given by

$$F = 2\pi \int_0^\theta I_D \sin\theta\, d\theta \qquad \text{(B-2)}$$

Combining equations (B-1) and (B-2) gives

$$F = 2\pi^3 a^4 \int_0^\theta \left[\frac{1}{\beta} J_1 (2\beta)\right]^2 \sin\theta\, d\theta \qquad \text{(B-3)}$$

From the definition of β we have

$$\sin\theta = \frac{2\beta}{\alpha} = \frac{\beta\lambda}{\pi a}$$

However, since preliminary calculations revealed that all angles involved in the diffraction pattern would be small; we have, approximately,

$$\theta = \frac{\beta\lambda}{\pi a} \qquad \text{(B-4)}$$

and $$d\theta = \frac{\lambda}{\pi a}\, d\beta \qquad \text{(B-5)}$$

Combining equations (B-3), (B-4), and (B-5), the approximate equation for the flux included within the angle θ becomes

$$F = 2\pi a^2 \lambda^2 \int_0^{\frac{\beta\lambda}{\pi a}} \left[\frac{1}{\beta} J_1(2\beta)\right]^2 \beta \, d\beta \qquad \text{(B-6)}$$

No attempt was made to integrate equation (B-6) analytically. The integrand, $f(\beta) = \beta\left[\frac{1}{\beta} J_1(2\beta)\right]^2$, was plotted against β for values of β from 0 to 14.52. This included nine diffraction rings of the diffraction pattern, and practically all of the diffracted flux is included within these nine rings. The total area under the curve was determined by planimeter. The areas under the curve from $\beta = 0$ to various values of β were also determined. For any value of β the ratio of the area to the total area gave the percentage of the diffracted flux included within the angle θ corresponding to that value of β.

The results are shown in graphical form in Figure II. For a given droplet radius and wavelength the percentage of the diffracted flux outside an angle θ can be computed.

For example, consider a droplet of 15 micron radius illuminated by blue light ($\lambda = 0.4$ microns). An aperture of .06" diameter is placed 20" from the particle along the line from the particle which is parallel to the incident light. It is desired to find the amount of diffracted flux which passes through the aperture. For this example we find

$$2\theta = \frac{.06}{20} = .003 \text{ radians}$$

$$\theta = .0015 \text{ radians}$$

$$\beta = \frac{\pi a \theta}{\lambda} = \frac{\pi \times 15 \times .0015}{.4} = .1768$$

Then from Figure II we find that 98% of the diffracted energy is excluded from the aperture, and 2% of the diffracted flux passes through the aperture.

APPENDIX C

Analysis of Optical System

In order to place the design of a photometric device for measuring particle size on a rational basis, it is first necessary to predict with some accuracy the angular distribution of the forward scattering of small particles. The analysis of this effect is contained in Appendix B. The second step is to devise a system which will separate as much of the scattered light as possible from that which is not scattered. In effect, this device may be thought of as a selective filter.

Previous investigators have found that most of the scattered light could be filtered out by observing the light transmission through an aperture at distances far from the scattering particles. Both Cheatham (3) and Sinclair (7,32) obtained a K_s of 2.0, which is equivalent to completely excluding the scattered light, at distances of the order of 18 feet. While it would be possible to design a laboratory instrument employing these distances by the use of reflecting mirrors or prisms to fold the light path back and forth, it would be much preferable to devise an instrument which could filter out the scattered light in a short distance . To accomplish this, the use of a collecting lens and a small aperture suggests itself.

In this appendix, an approximate analysis of such a system is presented, the object being to permit the selection of the significant parameters of the system geometry, and to permit

[illegible]

[illegible]

[illegible]

[illegible]

[illegible]

some estimation to be made of the percent of the scattered light which might be excluded. The assumptions inherent in this analysis are:

(1) That the principles of geometric optics will hold true
(2) That the focal points of the lenses and the light source are true points, of negligible area
(3) That the lenses may be considered thin
(4) That the light impinging on the lens is parallel
(5) That all the light passing through the small aperture will impinge on the photocell and be indicated

Consider the system shown in Figure VIII . The important components are :

(A) A single, spherical particle upon which a parallel beam of monochromatic light is incident
(B) A large aperture of diameter 2R, which limits the effective area of the lens
(C) A thin lens of relatively long focal length, f. All refractions of the light rays are assumed to occur in the plane of the lens
(D) A small aperture of diameter 2r, placed at the second focal point of lens (C)
(E) A photosensitive unit, which, through a suitable amplifier and meter will indicate the total amount of light energy impinging on the cell

All of the parallel light rays will pass through the second

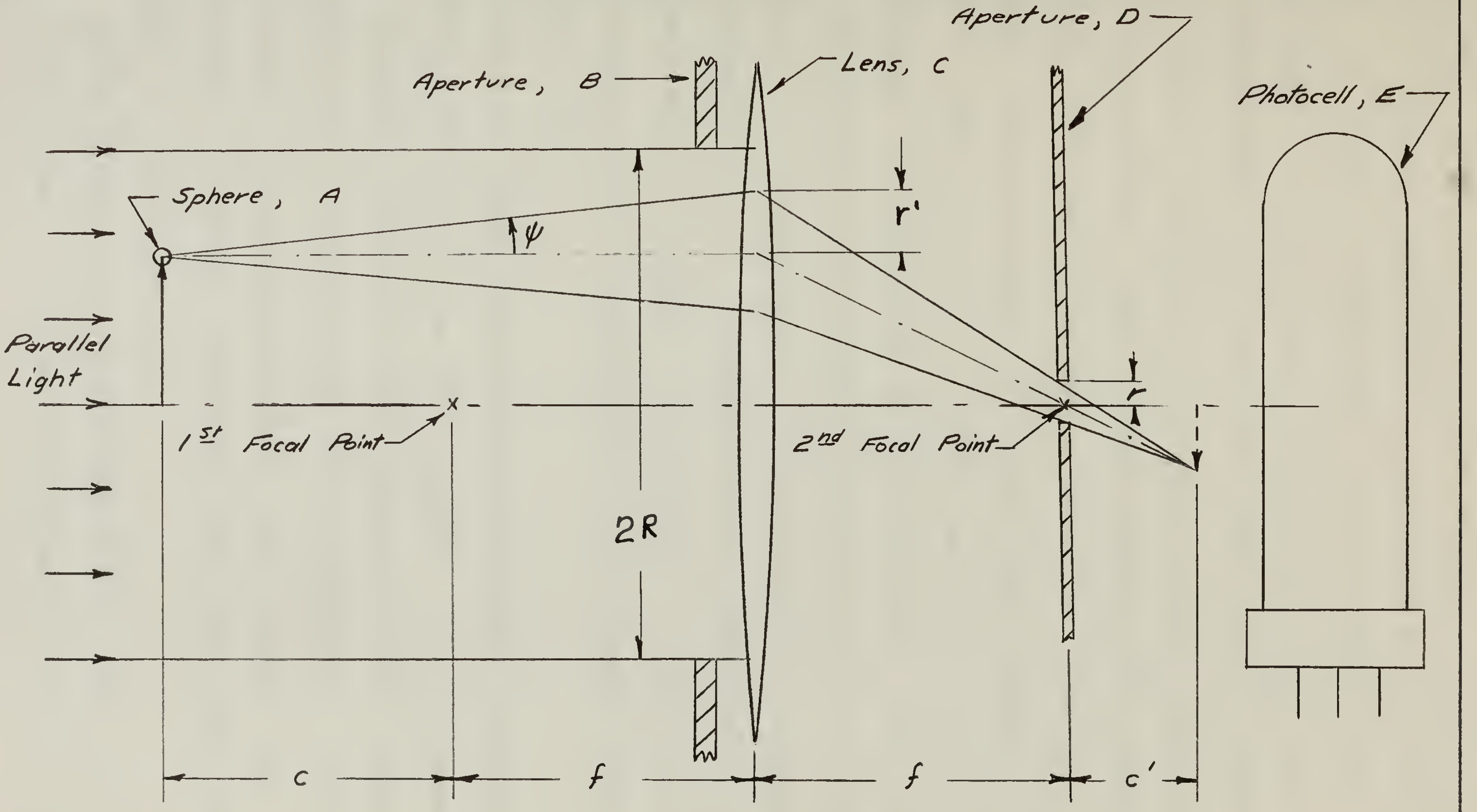

FIGURE VIII

OPTICAL SYSTEM

May 10, 1955 CFB

focal point of the lens and will impinge on the photosensitive cell, E, provided aperture D is as large as the light source image. It might be noted that, for an actual lens, this will be an image of finite area, rather than a true point.

Considering the diffracted light only, the spherical particle A may be visualized as a point source, emitting light rays in all directions. From the Mie theory we can predict the amount of energy radiated in any given direction. Referring to the diagram, only that amount of light energy included within the solid angle ω , represented by the plane angle ψ , will be captured by aperture D and measured by the photocell. We wish to predict just how much of the diffracted light we have succeeded in excluding from the photocell. It is therefore necessary to obtain an expression for ψ in terms of the system geometry. It is apparent that the smaller we can make ψ , the more successful our filter will be in separating the diffracted light from the parallel light.

The Mie theory may be used to determine the amount of energy included within any given solid angle. In the present case, we will consider only those solid angles which are symmetric about the direction of the parallel light propagation, and may therefore reduce our considerations to plane angles only. Thus the plane angle ψ actually represents the solid angle obtained by rotating ψ about its axis.

If the particle is located distance c from the first focal point of the lens, it may be considered as being a point on the

object shown as the solid arrow. From elementary optical theory, this object will be imaged by the lens at distance c' from the second focal point. The Newtonian lens equation gives for thin lenses the relationship between these distances as $cc' = f^2$.

Considering the particle at A as a point source, only those light rays which pass through apertures B and D will converge at the tip of the image. Now, assume that the distance r' will lie wholly within the large aperture B, that is, assume that the small aperture is controlling. Then the amount of diffracted light which impinges on the photocell will be that included within the angle ψ .

From similar triangles, $r/r' = c'/(f + c')$, or $r' = r(f + c')/c'$. From the lens equation, we have $c' = f^2/c$. Substituting, we get $r' = r(f + c)/f$. Now $\tan\psi = r'/(f + c) = r/f$. Therefore, as long as r' lies wholly with aperture B the amount of diffracted light captured is independent of distance, c, and independent of R. For this region we want r/f to be small, or a long focal length lens with a sharp focal point, to permit a small aperture, 2r.

Let us consider the other case, where the amount of diffracted light captured is limited only by the large aperture, rather than the small aperture. In this case, $r' = R$ and $\tan\psi = R/(f + c)$. This shows the important effect of distance c in making ψ small, as observed by Cheatham (3) and Sinclair (7,32).

Intermediate between these regions lies an area where the diffracted light is partially limited by the large aperture or

lens size and partially by the small aperture. In this range, the particle position relative to the central axis will affect the amount of diffracted light captured. A curve of the observed K_s versus c should appear somewhat as follows:

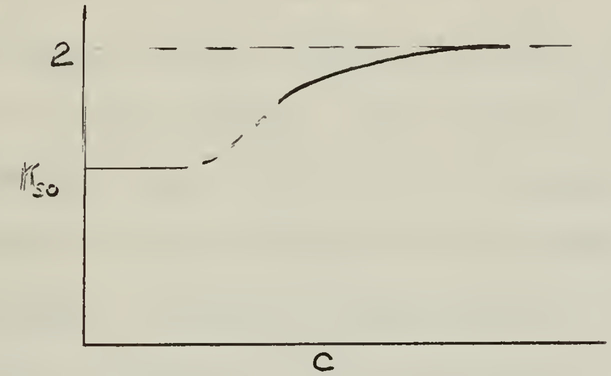

The dotted portion of the curve indicates the intermediate region. It is apparent that if r/f is sufficiently small, the initial portion of the curve can be made to approach 2. If this is practical it will not be necessary to go the long distances previously required experimentally by Cheatham and Sinclair.

APPENDIX D

Analysis of Data of Previous Investigators

The analyses presented in appendices "B" and "C" provide a method by which the performance of a given photometer may be predicted. Cheatham (3) had compiled a large amount of data using glass beads of known radius. For a given size of glass beads, a given aperture, and a given lens, Cheatham varied the distance from the sample to the photocell to determine the variation of K_{so} with distance. Several combinations of bead size, lenses and apertures were employed in the experiments.

For any of the experiments which were performed by Cheatham it is possible to predict the variation of K_{so} with distance. Calculations were made to compare the theoretical K_{so} with the values observed experimentally. Figures IX and X illustrate the results of these calculations for three of Cheatham's experiments. The agreement is considered satisfactory, and the decisions made relative to the selection of optical equipment were based on this agreement. (See Section II, Design of the Photometer).

As an example of how the predicted curves were calculated, consider the experiment using glass beads of 34 micron volume-surface mean diameter in oil, with a four inch focal length collecting lens and a one-sixteenth inch aperture. The phototube used was an RCA 1P39 with S4 spectral characteristics (peaks at 0.4 micron wave length). The lens diameter was five-eights inches (assumed as the diameter of the light beam). The distance from

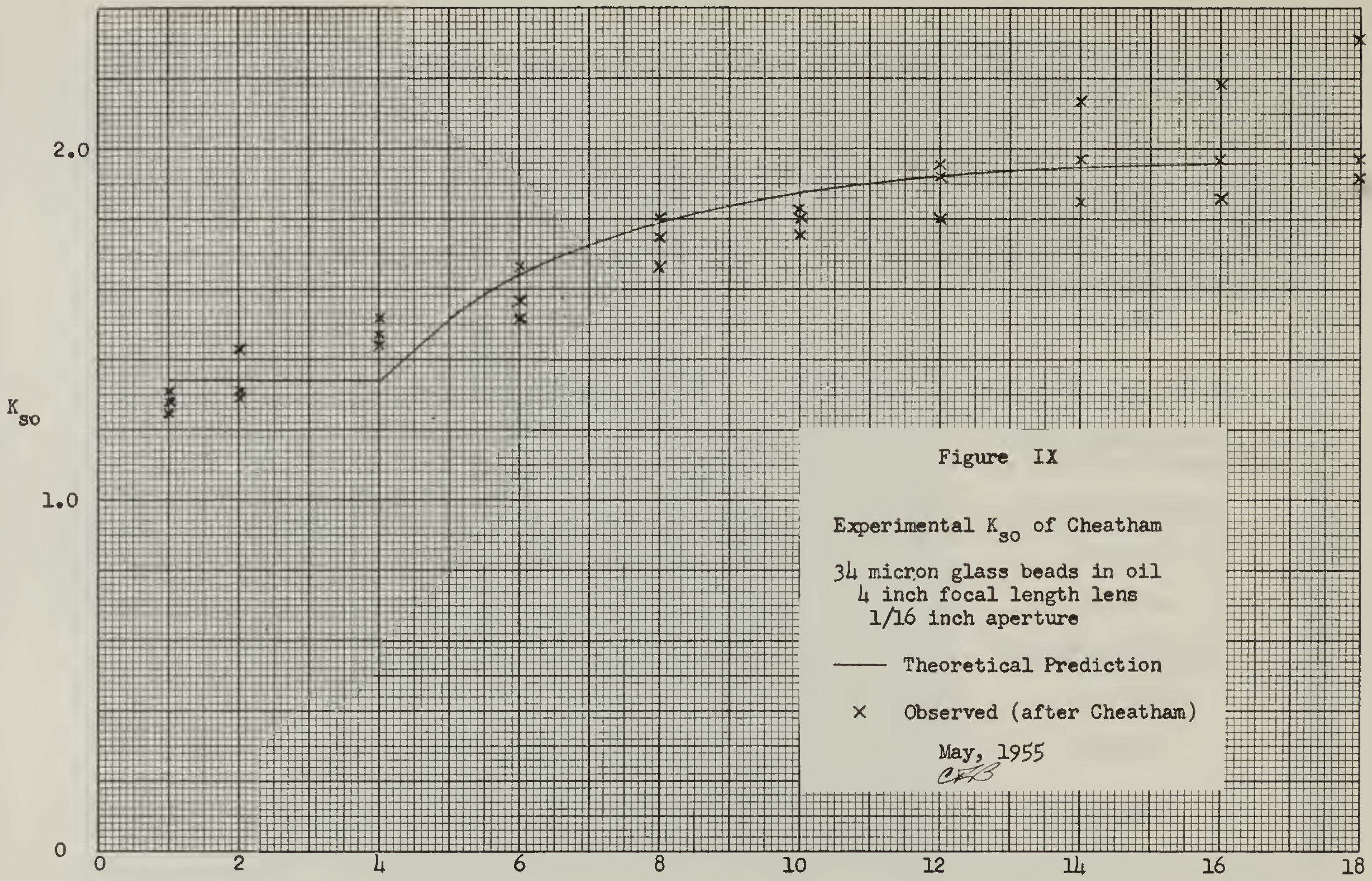

Figure IX

Experimental K_{so} of Cheatham

34 micron glass beads in oil
4 inch focal length lens
1/16 inch aperture

—— Theoretical Prediction

× Observed (after Cheatham)

May, 1955

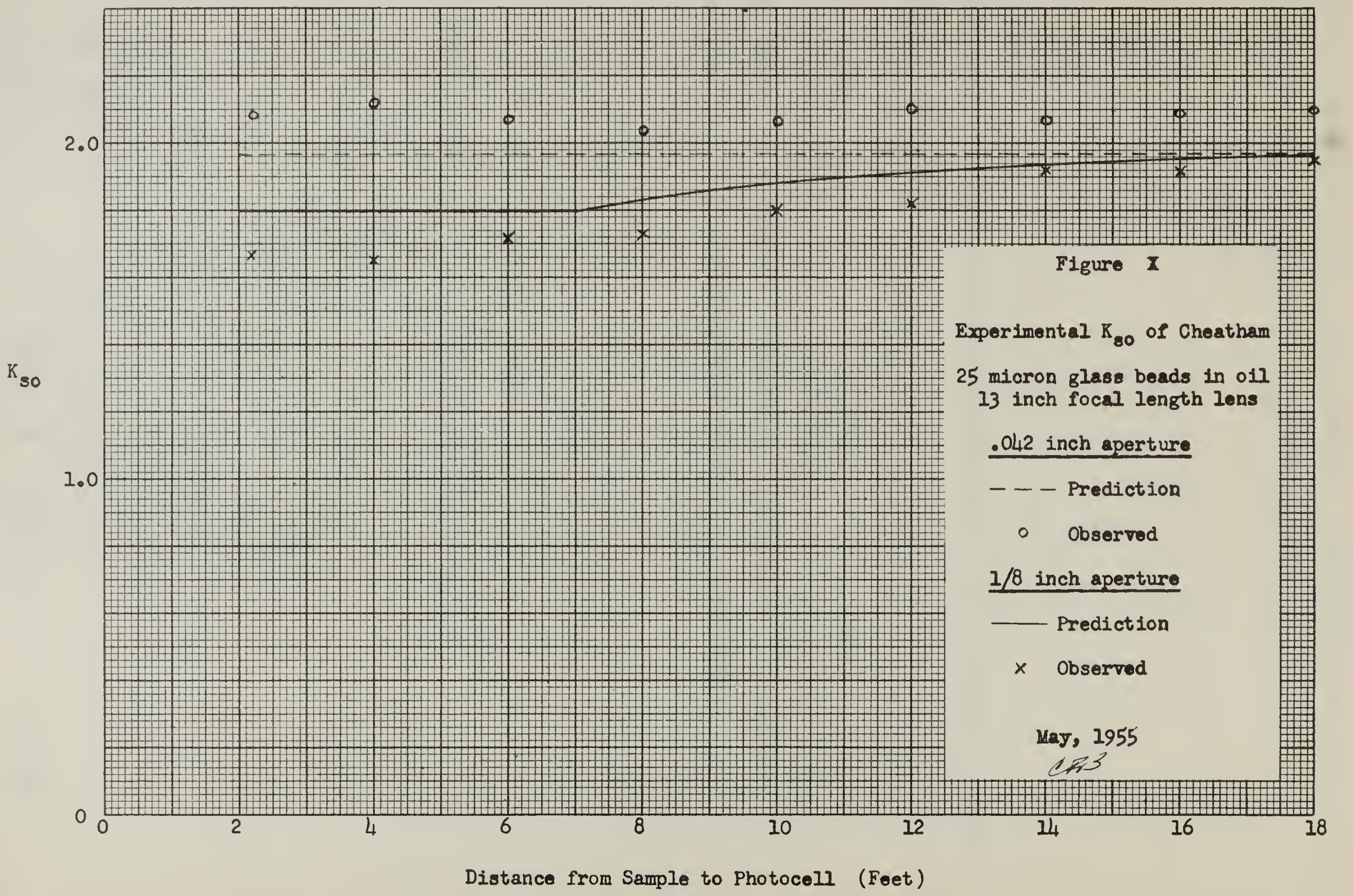

Figure X

Experimental K_{so} of Cheatham

25 micron glass beads in oil
13 inch focal length lens

May, 1955

aperture to phototube was four inches. Referring to Figure VIII, the values of the geometrical constants are :

$c = $ variable

$f = 4''$

$R = 5/16''$

$r = 1/32''$

$x = c + 2f + 4'' = c + 12''$

Following the procedure of Appendix C we find the limiting ψ for these constants to be

$$\text{Limiting } \psi = \frac{1}{32 \times 4} = .00781$$

and the value of c which corresponds to the dividing distance between aperture controlling and distance controlling is

$$\frac{R}{f + c} = \frac{r}{f}$$

$$c = \frac{fR}{r} - f = 36''$$

$$x = c + 12 = 48''$$

The optical constants for this experiment were:

$$\bar{a}_{\frac{3}{2}} = 17\,\mu$$

$$\lambda = 0.4\,\mu$$

$$\alpha = \frac{2\pi a}{\lambda} = 267$$

$$\beta = \frac{\pi a \theta}{\lambda} = 133.5\,\theta$$

When $x \leq 48''$; $\theta = \text{limiting } \psi = .00781$

When $x > 48''$; $\theta = \frac{R}{f + c} = \frac{R}{x + f - 12} = \frac{5/16}{x - 8}$

The predicted value of K_{so} is determined by calculating β for a given distance x and obtaining the percent diffracted energy excluded from the aperture from Figure II. The predicted value of K_{so} is then given by the expressions

$$K_{so} = 1 + \frac{\text{Percent Excluded}}{100}$$

For the present example, we have

$$x \leq 48''; \quad \beta = 133.5 \times .00781 = 1.045$$

$$\text{Percent excluded} = 34$$

$$K_{so} \text{ (observed)} = 1 + .34 = 1.34$$

$$x = 108''; \quad \theta = \frac{5/16}{108 - 8} = .00312$$

$$\beta = 133.5 \times .00312 = .418$$

$$\text{Percent excluded} = 83.5$$

$$K_{so} = 1 + .835 = 1.835$$

Additional points were obtained and the predicted curve is shown in Figure IX. Figure X illustrates the predicted curves for two additional experiments of Cheatham which illustrate the effect of a relatively long focal length for the collecting lens.

The agreement between the predicted values of K_{so} and the observed values was considered adequate enough to permit use of the analysis developed in Appendices "B" and "C" for the tentative design of a photometer. The conclusions arrived at in the preliminary design stage are discussed more fully in Section II, Design of the Photometer.

APPENDIX E

Linearity Check of Densichron

The linearity of the Densichron, with which all the light intensity measurements were taken, is an important factor in evaluating the experimental results. It is highly pertinent to establish that a change in light intensity which produces a change in density reading D from 0 to 0.2 will also produce an equal change in density reading at all ranges of the meter scale, say from 0.8 to 1.0.

With the optical bench and light source described in Section III, use can be made of the "Inverse Square Law" to check for linearity. Consider a point source of light, P. Let F represent the luminous flux crossing any section of a cone of solid angle ω steradians whose apex is at the source.

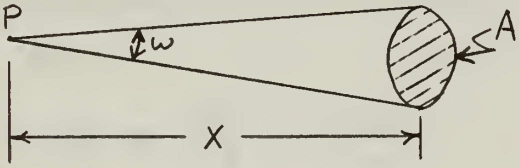

By definition, the luminous intensity of the source, I, is the ratio of the flux F to the solid angle ω .

$$I = \frac{F}{\omega}$$

Also by definition, a steradian is the solid angle subtended at the center of a sphere by an area of arbitrary shape on the surface of the sphere, equal to the square of the radius of

the sphere.

$$\omega = \frac{A}{x^2}$$

Combining these two relations, $F = \frac{IA}{x^2}$

The Densichron meter reading $D = \log_{10} \frac{1}{F}$. Taking the difference of two readings, D and D_o, substituting the expression for F, and converting to the natural system of logarithms, we have

$$D - D_o = \frac{1}{2.3}\left[\ln\left(\frac{x^2}{IA}\right) - \ln\left(\frac{x^2}{IA}\right)_o\right] = \frac{1}{2.3} \ln \frac{\left(\frac{x^2}{IA}\right)}{\left(\frac{x^2}{IA}\right)_o}$$

The luminous intensity I may be assumed to be constant, as we are looking at the light source from the same direction. The area A, which in the test procedure was a 1/2 inch aperture adjacent to the photosensitive unit, is also constant. Canceling these terms, we have

$$D - D_o = \frac{2}{2.3} \ln \frac{x}{x_o}$$

By adjusting the volume control of the Densichron to obtain a zero density reading at $x_o = 7.1$ inches, the formula can be reduced to

$$D = .869 \ln \frac{x}{7.1}$$

This is the relation which is shown plotted in Figure XI.

For a meter reading of 0 at x = 7.1, density readings were taken at various distances and are also shown plotted in Figure

[illegible]

$$[illegible]$$

[illegible]

[illegible]

$$[illegible]$$

[illegible]

$$[illegible]$$

[illegible]

$$[illegible]$$

[illegible]

XI. Readings were taken both with and without the blue filter in place. The observed data is contained in Table 2 .

The agreement of the experimental points with the theoretical line is considered excellent. No corrections to any of the subsequent Densichron readings were considered necessary.

The linearity check was carried out in a darkroom, and at first some difficulty was experienced with light reflected from the darkroom walls. The photocell behind the aperture effectively "saw" more of the reflected light from the walls as the distance from the light source was increased. This difficulty was overcome by shielding the light source with a black cloth in all directions except that in which the photocell was located. Thus, the only light impinging on the walls was in back of the photocell, and could not be "seen" by it except through secondary reflections, which were negligible.

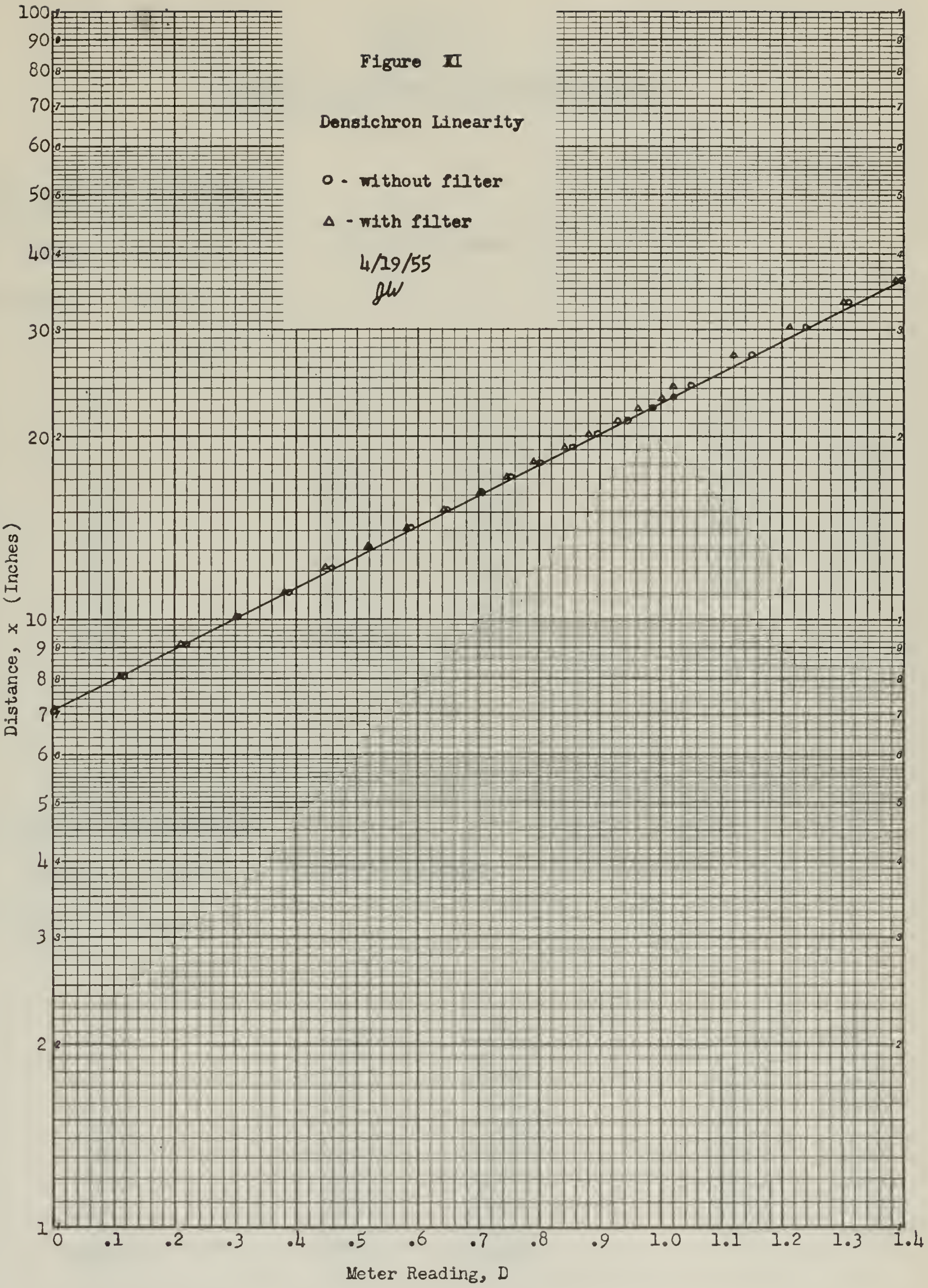

Figure XI

Densichron Linearity

o - without filter

Δ - with filter

4/19/55
JW

TABLE 2

Linearity Check of Densichron

Filter not in system

Light source current: 110 milliamps

Densichron: Range 2

Volume 7

x	D	x	D	x	D
7.1	0	15.1	.650	23.1	1.02
8.1	.115	16.1	.705	24.1	1.05
9.1	.220	17.1	.755	27.1	1.15
10.1	.305	18.1	.800	30.1	1.24
11.1	.385	19.1	.855	33.1	1.31
12.1	.460	20.1	.895	36.1	1.40
13.1	.520	21.1	.945		
14.1	.590	22.1	.985		

Blue filter in system

Light source current: 140 milliamps

Densichron: Range 2

Volume 7

x	D	x	D	x	D
7.1	0	15.1	.640	23.1	1.00
8.1	.110	16.1	.695	24.1	1.02
9.1	.210	17.1	.745	27.1	1.12
10.1	.300	18.1	.785	30.1	1.21
11.1	.380	19.1	.835	33.1	1.30
12.1	.445	20.1	.880	36.1	1.39
13.1	.515	21.1	.925	39.1	1.42
14.1	.580	22.1	.960		

APPENDIX F

Measurement of Experimental Constants

The following experimental constants were determined in connection with the calibration of the photometer:

(1) Volume-surface mean diameter of two grades of glass beads.

(2) Density of glass beads.

(3) Density of oil used as suspending medium for glass beads in test cell.

Measurement of Volume-Surface Mean Diameter of Glass Beads

Photomicrographs were taken of the two grades of glass beads used for calibration purposes. For this purpose a Bausch and Lomb illuminating microscope was used with a 15X ocular, 32 mm objective and no condensing lens. A mixture of Nujol oil and glass beads was spread on a glass slide, focus obtained on the microscope and in the camera. Four photomicrographs of each grade of beads were taken and one photomicrograph of a slide micrometer was taken with the same magnification. The prints were made using an enlarger which provided a total magnification of about 1600X.

A transparent graticule was used to measure the number of beads smaller than certain diameters. The data obtained is summarized in Tables 3 and 4 and is plotted in Figures XII and XIV, which show the percentage of beads smaller

than a given diameter versus the diameter. The distribution curve for each grade of beads is obtained by finding the derivative curves for Figures XII and XIV. The distribution curves for the two grades of beads are shown in Figures XIII and XV. The volume-surface mean diameter is obtained from the distribution curve by use of the definition

$$\bar{d}_{\frac{3}{2}} \equiv \frac{\int d^3 \quad G \quad dd}{\int d^2 \quad G \quad dd} \qquad \text{(F-1)}$$

where $G \equiv \frac{dn}{dd}$

The calculations to evaluate the integrals indicated in Equation (F-1) were made using Simpson's first rule of approximate integration. These calculations are shown in Tables 5 and 6

TABLE 3

Photomicrograph Measurement of 3M Superbrite Beads, Type 119, 35-C-7412, Serial 3364, manufactured by the Minnesota Mining and Manufacturing Company; from photomicrographs taken April 11, 1955.

	Diameter Smaller Than (Microns)									
Picture No.	6	12	17	23	28	34	39	44	50	56
1	0	2	28	95	158	198	210	215	215	215
2	0	5	44	119	187	205	217	219	219	219
3	0	4	46	121	179	213	220	221	221	221
4	0	2	42	132	203	240	252	255	256	256
Totals	0	13	160	467	727	856	899	910	911	911
Percentage	0	1.4	17.5	51.2	79.8	94.0	98.6	99.9	100	100

(See Figure XII for plot.)

TABLE 4

Photomicrograph Measurement of 3M Superbrite Glass Beads, Type 119, 35C-4762, Serial 3357, manufactured by the Minnesota Mining and Manufacturing Company, from photomicrographs taken April 11, 1955.

	Diameter Smaller than (Microns)									
Picture No.	5	11	16	22	27	33	37	43	49	54
1	0	0	3	19	50	80	97	111	116	117
2	0	4	26	67	107	141	155	160	160	161
3	0	2	18	57	93	117	128	132	132	132
4	0	0	7	20	39	65	80	86	87	87
Total	0	6	54	163	289	403	460	489	495	497
Percentage	0	1.21	10.87	32.8	58.2	81.3	92.5	98.5	99.6	100

(See Figure XIV for plot.)

TABLE 5

Calculation of $\bar{d}_{\frac{3}{2}}$ for 3 Beads, Type 119, 35C-7412, Serial 3364

Diameter	G	$d^2 G$	S.M.	$f(d^2 G)$	$f(d^3 G)$
5	0	0	1	0	0
10	.158	15.8	4	64	632
15	1.555	350	2	700	10500
20	2.83	1132	4	4528	90560
25	2.83	1769	2	3538	88450
30	1.26	1134	4	4536	136080
35	.51	625	2	1250	43750
40	.21	336	4	1344	53760
45	0	0	1	0	0
			Totals	15960	423732

$$\bar{d}_{\frac{3}{2}} = \frac{\sum f(d^3 G)}{\sum f(d^2 G)} = \frac{423{,}732}{15960} = 26.6 \text{ Microns}$$

TABLE 6

Calculation of $\bar{d}_{\frac{3}{2}}$ for 3M Beads, Type 119, 35C-4762, Serial 3357

Diameter	G	d^2 G	S.M.	$f(d^2 G)$	$f(d^3 G)$
5	0	0	1	0	0
10	.25	25	4	100	1000
15	1.15	259	2	518	7770
20	2.20	880	4	3520	70400
25	2.53	1581	2	3162	79050
30	2.18	1962	4	7848	235440
35	1.38	1690	2	3380	118300
40	.53	848	4	3392	135680
45	.12	243	2	486	21870
50	.04	100	4	400	20000
55	0	0	1	0	0
			Totals	22806	689510

$$\bar{d}_{\frac{3}{2}} = \frac{\sum f(d^3 \; G)}{\sum f(d^2 \; G)} = \frac{689510}{22806} = 30.1 \text{ Microns}$$

Determination of Density of Glass Beads

This constant was determined by the simple procedure of measuring the displacement in water of a measured weight of beads. A standard 50ml graduate was used to measure volumes, and a chemical balance to measure weights. The beads were stirred thoroughly after being put in the graduate to remove any entrapped air. Two independent measurements were made, one yielding a density of 2.42 gm/cm^3, and the other 2.415 gm/cm^3.

[illegible]

[illegible]

[illegible]

[illegible]

[illegible]

[illegible]

Determination of Density of Oil

The oil used to suspend the glass beads in was Dow-Corning 550 (Silicone) oil. This oil had been selected by Cheatham (3) because of its ability to prevent agglomeration of the glass beads. The density of the oil was found to be 1.076 grams/cc by use of a specific gravity bottle.

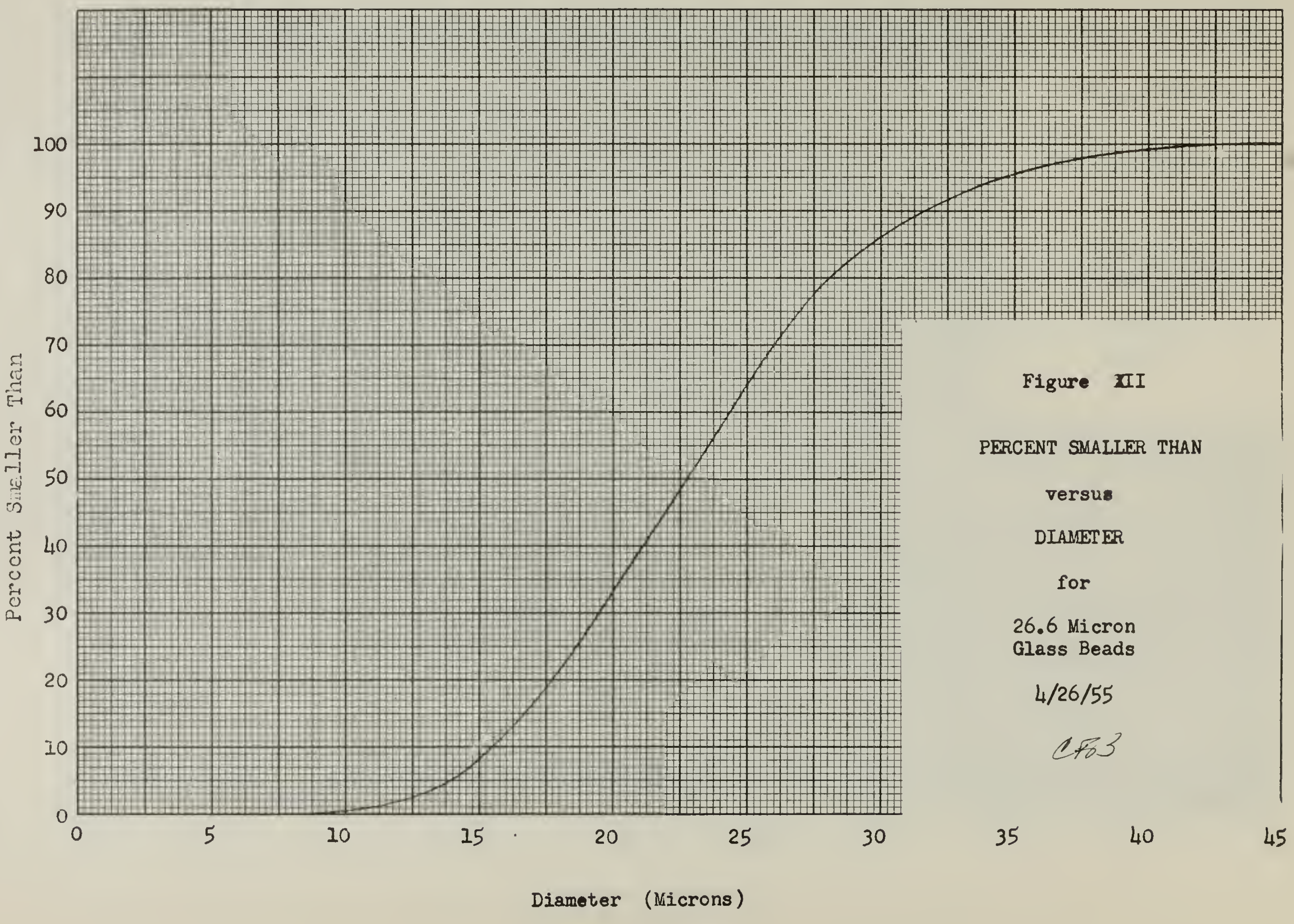

Figure XII

PERCENT SMALLER THAN

versus

DIAMETER

for

26.6 Micron
Glass Beads

4/26/55

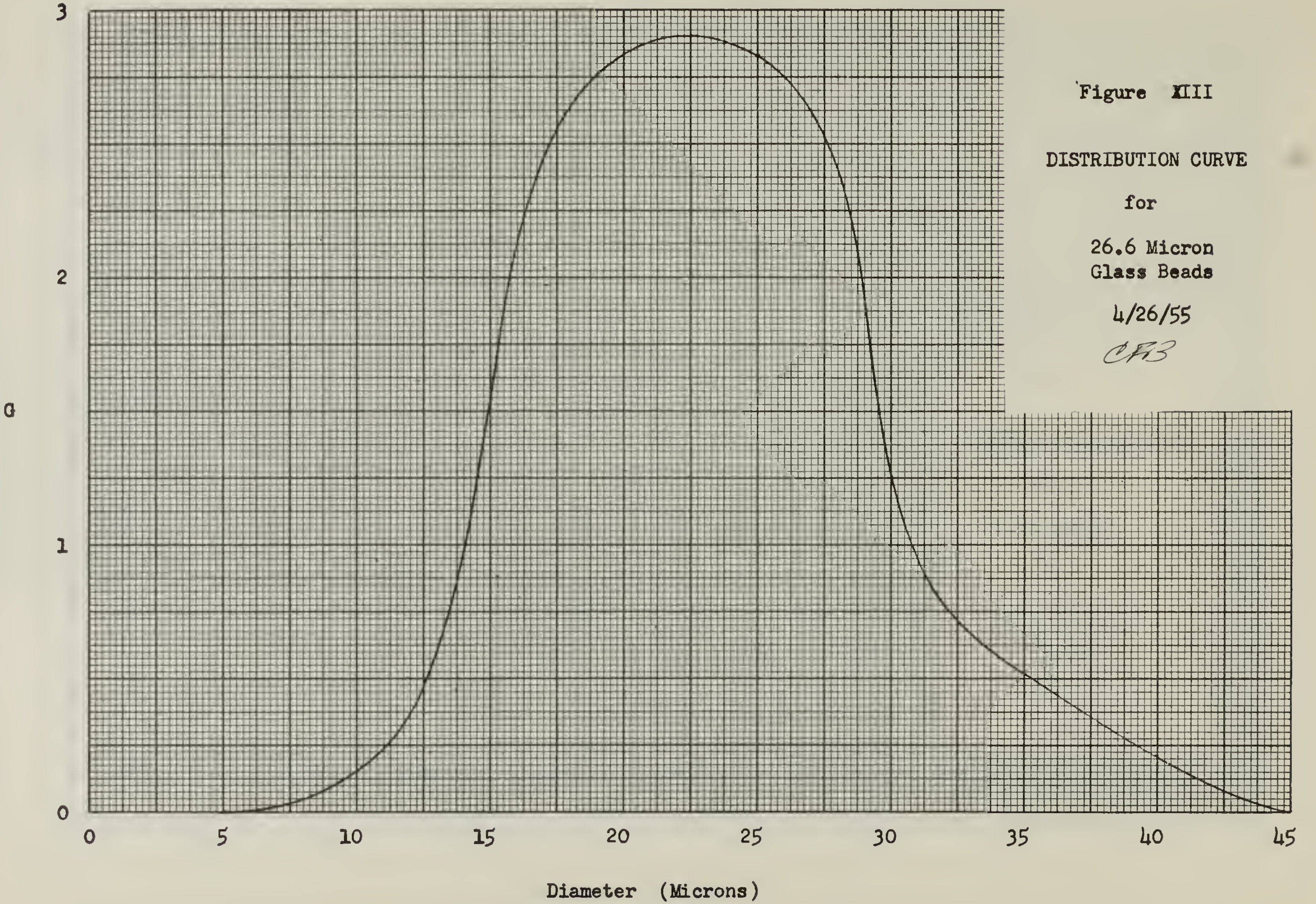

Figure XIII

DISTRIBUTION CURVE

for

26.6 Micron
Glass Beads

4/26/55

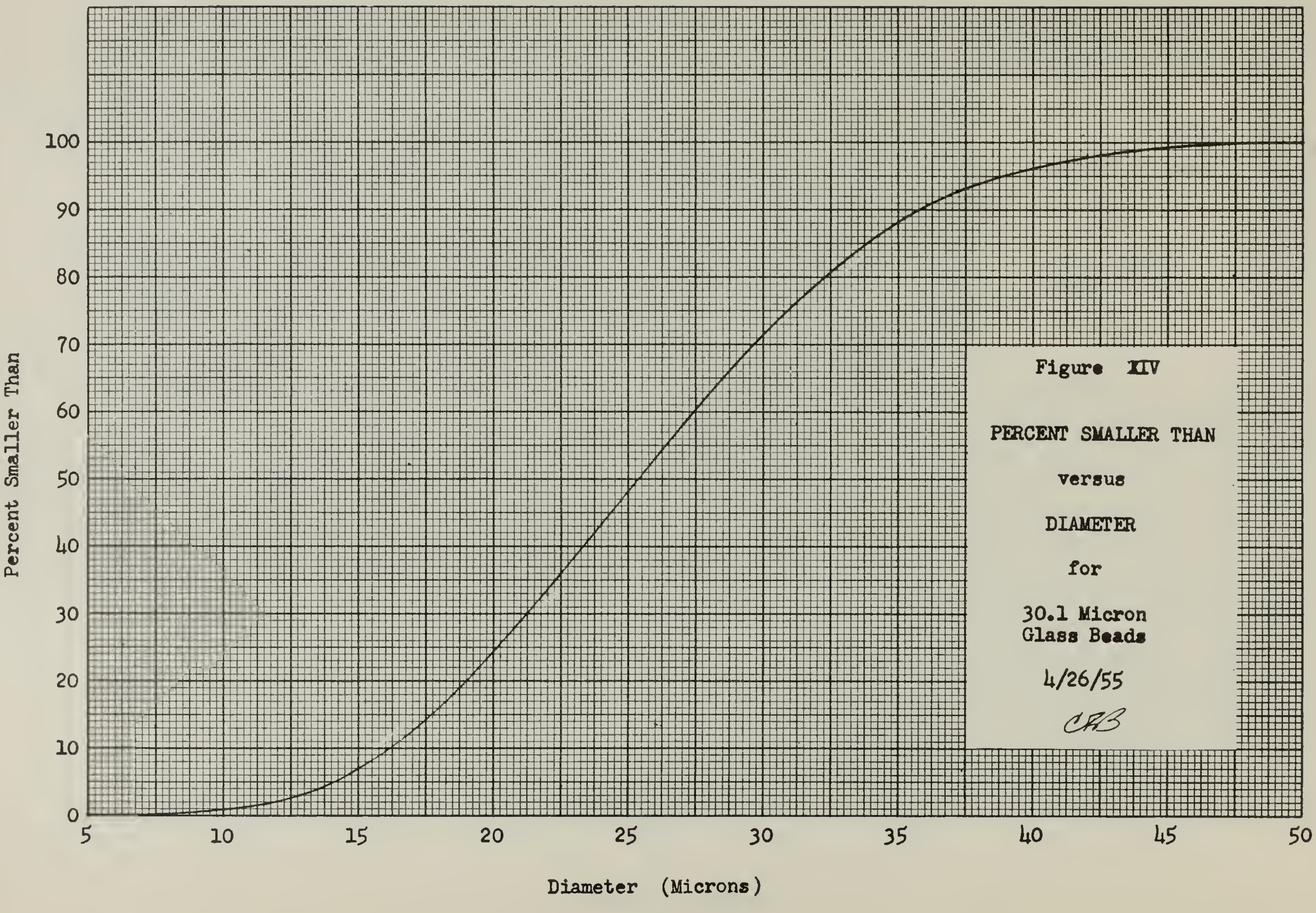

Figure XIV

PERCENT SMALLER THAN

versus

DIAMETER

for

30.1 Micron
Glass Beads

4/26/55

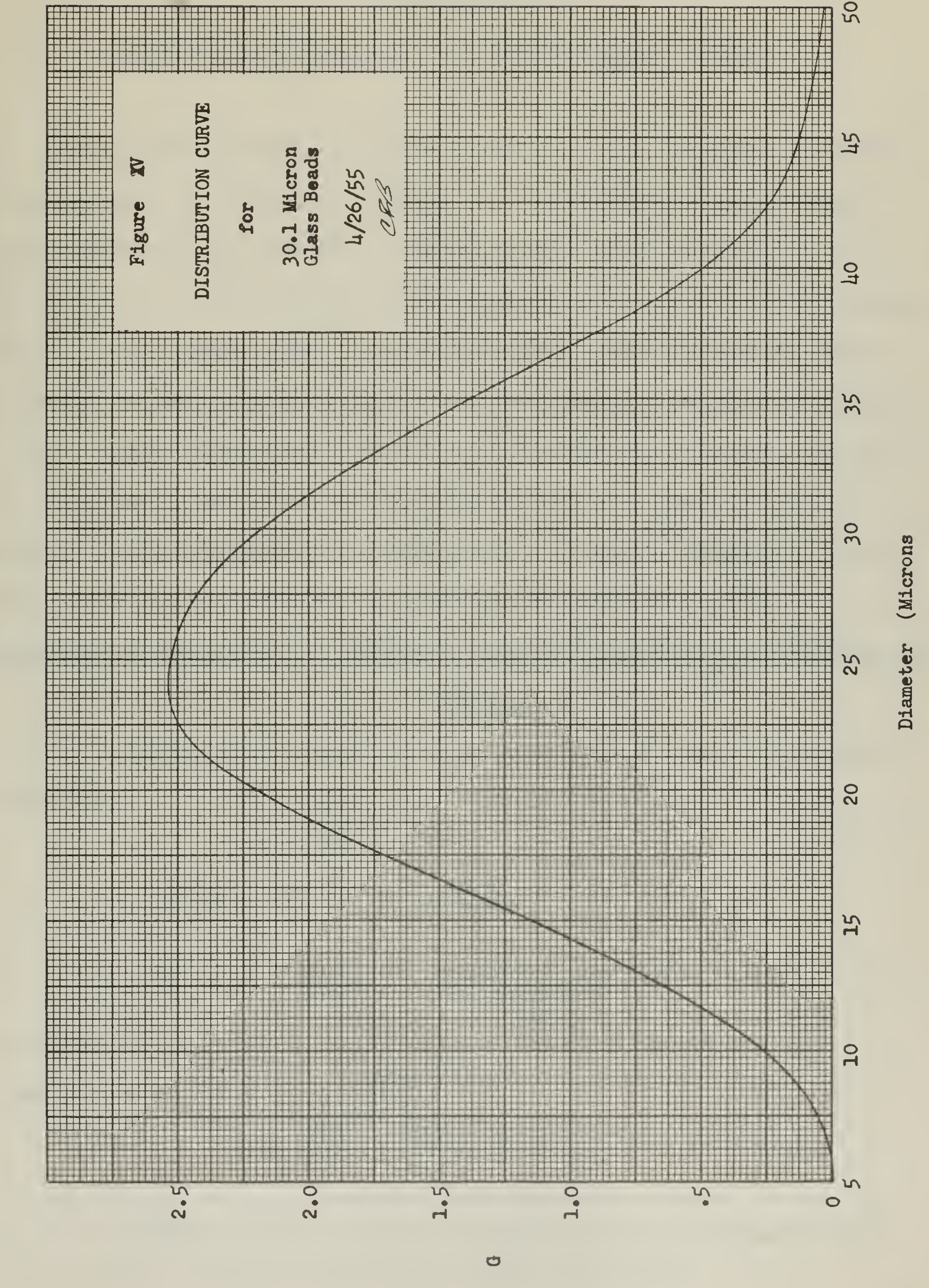

Figure XV

DISTRIBUTION CURVE

for

30.1 Micron
Glass Beads

4/26/55

APPENDIX G

Governing Equations for Atomization Studies

Atomization studies will be performed on a system in which particles will be carried through the photometer light beam by a high velocity air stream. By measuring the decrease in intensity of the light due to the passage of the particles, a measurement of particle size can be obtained. The following derivations were made specifically for the dynamic calibration runs, in which glass beads were injected into the air stream, but will also be equally applicable to atomization of water by an air stream. The apparatus for entraining the glass beads in an air stream is fully described by Gottling in reference (39).

Transmission Equation for Beads or Water Droplets in a Moving Air Stream

The transmission equation (see Appendix A) may be arranged in the form

$$\mathrm{Ln}\ \frac{E_o}{E} = Snl \qquad \text{(G-1)}$$

where $S = K_{so} \dfrac{\pi d^2}{4}$

and n = number of particles per unit volume of the mixture

The number of particles in an aerosol moving through a unit volume at velocity V is given by

$$n = \frac{w_b}{AV} \times \frac{6}{\pi d^3 \rho_b}$$

where $\dfrac{w_b}{AV}$ may be thought of as the spatial density of the particles, in lb/ft^3

[illegible]

[illegible]

[illegible]

[illegible]

[illegible]

$$[illegible]$$

[illegible]

$$[illegible]$$

[illegible]

[illegible]

$$[illegible]$$

[illegible]

Substituting the expressions for S and n into equation (G-1), the transmission equation becomes

$$\ln \frac{E_o}{E} = \frac{3 \; K_{so} \; \bar{w}_b \; l}{2 \, A V \, d \, \rho_b} \qquad \text{(G-2)}$$

Solving for the diameter d and substituting 2.303$(D-D_o)$ for its equivalent $\ln E_o/E$ (see Section III), the following expression for particle diameter is obtained

$$d = \frac{3 \; K_{so} \; \bar{w}_b \; l}{2 \, A V \rho_b \cdot 2.303 (D - D_o)} \qquad \text{(G-3)}$$

For a predicted value of K_{so}, equation (G-3) gives the particle size in terms of system constants and quantities which may be determined experimentally. In order to apply this equation, it is necessary to develop an expression for velocity in terms of measureable quantities. This is done in the following paragraphs.

Particle Velocity at Photometer

The system considered is shown below.

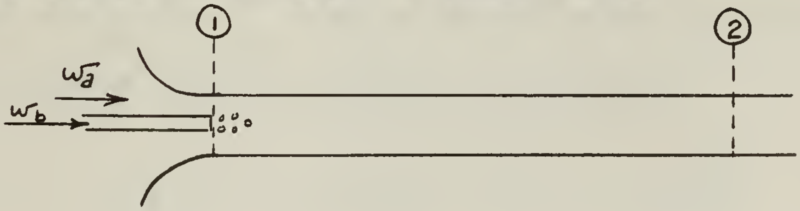

It will be assumed that the velocity of the beads is negligible at section 1, and that the velocity of the beads is the same as that of the air stream at section 2. The latter

assumption has been found to be very nearly true for water droplets in air as the large drag forces on the particles cause them to accelerate quite rapidly. It is estimated that the particles reach essentially main stream velocity within a foot or two of the point of injection. The photometric measurements were taken approximately five feet downstream of the point of bead injection.

The Steady Flow Energy Equation for adiabatic flow between sections 1 and 2 may be written as

$$\bar{w}_a h_{a_1} + \bar{w}_a \frac{V_{a_1}^2}{2g} + \bar{w}_b h_{b_1} + \bar{w}_b \frac{V_{b_1}^2}{2g} = \bar{w}_a h_{a_2} + \bar{w}_a \frac{V_{a_2}^2}{2g} + \bar{w}_b h_{b_2} + \bar{w}_b \frac{V_{b_2}^2}{2g} \qquad \text{(G-4)}$$

Employing the assumptions made in the above paragraph and further assuming that heat transfer effects between the air stream and the beads are negligible so that $h_{b_1} = h_{b_2}$, equation (G-4) reduces to

$$\bar{w}_a h_{a_1} + \bar{w}_a \frac{V_{a_1}^2}{2g} = \bar{w}_a h_{a_2} + (\bar{w}_a + \bar{w}_b) \frac{V_2^2}{2g}$$

where $V_2 = V_{a_2} = V_{b_2}$. Using the definition of stagnation enthalpy for the air at section 1, we obtain

$$\bar{w}_a h_{a_{01}} = \bar{w}_a h_{a_2} + (\bar{w}_a + \bar{w}_b) \frac{V_2^2}{2g} \qquad \text{(G-5)}$$

Introducing the perfect Gas Law for air and rearranging,

$$\left(1 + \frac{\bar{w}_b}{\bar{w}_a}\right) \frac{V_2^2}{2g} + c_p (T_2 - T_{01}) = 0 \qquad \text{(G-6)}$$

Noting that the volume rate of flow of the beads will be at least 2 orders of magnitude less than that of air, the continuity equation for the air flow may be written as:

$$\frac{w_a}{A} = \rho_2 V_2 = \frac{P_2}{R T_2} V_2 \qquad \text{(G-7)}$$

Solving for T_2:

$$T_2 = \frac{P_2 V_2}{R} \times \frac{A}{w_a}$$

Substituting this expression for T_2 into equation (G-6), we have

$$\left(1 + \frac{w_b}{w_a}\right) \frac{V_2^2}{2g} + C_p \frac{P_2}{R} \frac{A}{w_a} V_2 - C_p T_{01} = 0 \qquad \text{(G-8)}$$

This equation contains V_2 in terms of constants, measurable quantities, and the mass rate of flow of air.

Mass Rate of Air Flow

The bell shaped nozzle at the inlet to the test section provides a convenient means for the determination of the air flow rate if isentropic flow is assumed. In equation (4.16) of reference (37), the mass flow per unit area is given in terms of the Mach Number as

$$\frac{w_a}{A} = \sqrt{\frac{k}{R}} \, \frac{P_0}{\sqrt{T_0}} \, \frac{M}{\left(1 + \frac{k-1}{2} M^2\right)^{\frac{k+1}{2(k-1)}}} \qquad \text{(G-9)}$$

[illegible]

$$[illegible]$$

[illegible]

$$[illegible]$$

[illegible]

$$[illegible]$$

[illegible]

$$[illegible]$$

[illegible]

$$[illegible]$$

The ratio of the actual area to the area required for sonic velocity is given by:

$$\frac{A}{A^*} = \frac{1}{M}\left[\left(\frac{2}{k+1}\right)\left(1+\frac{k-1}{2}M^2\right)\right]^{\frac{k+1}{2(k-1)}} \tag{G-10}$$

Eliminating M between equations (G-9) and (G-10),

$$\frac{w_a}{A} = \sqrt{\frac{k}{R}}\;\frac{p_o}{\sqrt{T_o}}\left[\frac{2}{k+1}\right]^{\frac{k+1}{2(k-1)}} \cdot \frac{A^*}{A} \tag{G-11}$$

The quantity A/A* is a function only of the pressure ratio p/p_o and is tabulated in the Gas Tables (38). Therefore, knowing the area of the nozzle throat, and assuming isentropic flow in the nozzle, the mass rate of flow of air can be obtained from the measured static pressure at the throat and the stagnation pressure.

[illegible]

$$[illegible]$$

[illegible]

$$[illegible]$$

[illegible]

Appendix H

Original Data

TABLE 7

Run No. 4 April 1, 1955

Glass Beads in oil.

$\bar{d}_{\frac{3}{2}}$ = 30.1 microns

Focal length (f) = 19.8"

Aperture Diameter (2r) = .0625"

Weight of oil (W) = 51.5 gms.

Weight of beads (w) = .0351 grams

Distance - aperture to photocell = 5.6 inches

Position of collecting lens = 45.3"

$K_{so} = .00411 \frac{W}{w} (D-D_o) = 6.03 (D-D_o)$

x	f + c	2R	$\frac{f+c}{R}$	D_o	D	$D-D_o$	K_{so}
36"	9.3"	25mm	18.9	.01	.355	.345	2.08
33	12.3	25	25.0	.01	.355	.345	2.08
30	15.3	25	31.1	.01	.355	.345	2.08
27	18.3	25	37.2	.01	.355	.345	2.08
24	21.3	25	43.0	.005	.355	.350	2.11
20	25.3	25	51.4	.005	.355	.350	2.11
16	29.3	25	59.6	.005	.36	.355	2.14
36	9.3	20	23.6	.01	.36	.35	2.11
33	12.3	20	31.2	.01	.36	.35	2.11
30	15.3	20	38.8	.01	.36	.35	2.11
27	18.3	20	46.4	.01	.355	.345	2.08
24	21.3	20	54.0	.01	.355	.345	2.08
20	25.3	20	64.2	.005	.355	.350	2.11
16	29.3	20	74.4	.005	.355	.350	2.11
36	9.3	15	31.7	0	.345	.345	2.08
33	12.3	15	41.6	0	.345	.345	2.08
30	15.3	15	51.8	0	.345	.345	2.08
27	18.3	15	62.0	0	.34	.34	2.05
24	21.3	15	72.2	0	.34	.34	2.05
20	25.3	15	85.6	0	.34	.34	2.05
16	29.3	15	99.2	0	.34	.34	2.05
36	9.3	10	47.2	0	.345	.345	2.08
33	12.3	10	62.4	0	.345	.345	2.08
30	15.3	10	77.8	0	.345	.345	2.08
27	18.3	10	93.0	0	.34	.34	2.05
24	21.3	10	108.4	0	.34	.34	2.05
20	25.3	10	128.6	0	.34	.34	2.05
16	29.3	10	149.0	0	.34	.34	2.05

TABLE 8

Run No. 5 April 2, 1955
Glass beads in oil.
$\bar{d}_{\frac{3}{2}}$ = 30.1 microns
Focal length (f) = 12.4"
Aperture diameter (2r) = .0200"
Weight of oil (W) = 51.5 grams
Weight of beads (w) = .0351 grams
Distance - aperture to photocell = 3.4"
Position of collecting lens = 52.5"
$K_{so} = .00411 \quad \frac{W}{w}(D-D_o) = 6.03\ (D-D_o)$

x	f + c	2R	$\frac{f+c}{R}$	D_o	D	$D-D_o$	K_{so}
42"	10.5"	25mm	21.3	.46	.98	.52	3.13
39	13.5	25	27.4	.465	.975	.51	3.08
36	16.5	25	33.5	.465	.97	.505	3.05
33	19.5	25	39.6	.465	.97	.505	3.05
30	22.5	25	45.7	.46	.97	.51	3.08
27	25.5	25	51.8	.46	.97	.51	3.08
24	28.5	25	57.9	.46	.97	.51	3.08
20	32.5	25	66.1	.455	.97	.515	3.10
16	36.5	25	74.3	.455	.97	.515	3.10
42	10.5	20	26.7	.455	.975	.52	3.13
39	13.5	20	34.3	.45	.97	.52	3.13
36	16.5	20	41.9	.45	.965	.515	3.10
33	19.5	20	49.5	.445	.965	.52	3.13
30	22.5	20	57.2	.445	.965	.52	3.13
27	25.5	20	64.8	.445	.965	.52	3.13
24	28.5	20	72.4	.44	.965	.525	3.16
20	32.5	20	82.6	.435	.965	.53	3.19
16	36.5	20	92.6	.43	.965	.535	3.22
42	10.5	15	35.6	.49	.98	.49	2.96
39	13.5	15	45.7	.485	.975	.49	2.96
36	16.5	15	55.9	.48	.97	.49	2.96
33	19.5	15	66.1	.475	.96	.485	2.93
30	22.5	15	76.2	.47	.96	.49	2.96
27	25.5	15	86.5	.46	.955	.495	2.98
24	28.5	15	96.6	.455	.95	.495	2.98
20	32.5	15	110.0	.445	.945	.500	3.01
16	36.5	15	123.7	.43	.945	.515	3.10

TABLE 9

Run No. 8 April 8, 1955
Glass Beads in oil
$\bar{d}_{\frac{3}{2}}$ = 26.6 microns
Focal length (f) = 18.5"
Aperture diameter (2r) = .0400"
Weight of oil (W) = 51.0 gms.
Weight of beads (w) = .0319 grms
Distance-aperture to photocell = 6.0"
Position of collecting lens = 47.1"
$K_{so} = .00364 \frac{W}{w} (D-D_o) = 5.82 (D-D_o)$

x	f + c	2R	$\frac{f+c}{R}$	D_o	D	$D-D_o$	K_{so}
36"	11.1"	20mm	28.2	.183	.603	.42	2.45
33	14.1	20	35.8	.18	.598	.418	2.43
30	17.1	20	43.4	.175	.59	.415	2.41
27	20.1	20	51.0	.165	.583	.418	2.43
24	23.1	20	58.6	.16	.578	.418	2.43
20	27.1	20	68.8	.158	.578	.42	2.45
16	31.1	20	78.9	.155	.578	.423	2.46

TABLE 10

Run No. 11
Glass Beads in oil
Focal length (f) = 19.1"
Aperture diameter (2r) = .0400"
Weight of beads (w) = .0410 gms
Distance-aperture to photocell = 5.9"
Position of collecting lens - 46.5"

April 13, 1955
$\bar{d}_{\frac{3}{2}}$ = 30.1 microns
Weight of oil (W) = 49.5gms

$K_{so} = .00411 \frac{W}{w} (D-D_o) = 4.96 (D-D_o)$

x	f + c	2R	$\frac{f+c}{R}$	D_o	D	$D-D_o$	K_{so}
36"	10.5"	16mm	33.4	.055	.543	.488	2.42
33	13.5	16	42.9	.053	.548	.495	2.45
30	16.5	16	52.5	.06	.558	.498	2.47
27	19.5	16	62.0	.065	.563	.498	2.47
24	22.5	16	71.5	.08	.585	.505	2.50
20	26.5	16	84.2	.10	.613	.513	2.54
16	30.5	16	97.0	.125	.645	.520	2.58

TABLE 11

Run No. 12
Glass Beads in Oil
Weight of oil (W) = 52.4 gms
Weight of beads (w) = .0406 gms
$K_{so} = .00364 \frac{W}{w} (D-D_o) = 4.70(D-D_o)$
Other data same as Run No. 11

April 15, 1955
$\bar{d}_{\frac{3}{2}}$ = 26.6 microns
Aperture = .0400"

x	f + c	2R	$\frac{f+c}{R}$	D_o	D	$D-D_o$	K_{so}
36"	10.5"	20mm	26.7	.06	.56	.50	2.35
33	13.5	20	34.3	.06	.56	.50	2.35
30	16.5	20	41.9	.06	.56	.50	2.35
27	19.5	20	49.6	.06	.56	.50	2.35
24	22.5	20	57.2	.06	.56	.50	2.35
20	26.5	20	67.3	.06	.57	.51	2.39
16	30.5	20	77.5	.065	.58	.515	2.42

TABLE 12

Run No. 13
Glass Beads in oil
Weight of oil (W) = 51.4 gms
Weight of beads (w) = .0355 gms
$K_{so} = .00364 \frac{W}{w} (D-D_o) = 5.26 (D-D_o)$
Other data same as Run No. 11

April 15, 1955
$\bar{d}_{\frac{3}{2}}$ = 26.6 microns
Aperture dia. = .0400"

x	f + c	2R	$\frac{f+c}{R}$	D_o	D	$D-D_o$	K_{so}
36"	10.5"	20mm	26.7	.105	.56	.455	2.39
33	13.5	20	34.3	.105	.56	.455	2.39
30	16.5	20	41.9	.105	.563	.458	2.41
27	19.5	20	49.6	.105	.568	.463	2.43
24	22.5	20	57.2	.11	.573	.463	2.43
20	26.5	20	67.3	.115	.588	.473	2.49
16	30.5	20	77.5	.12	.603	.483	2.54

TABLE 13

Run No. 14
Glass Beads in oil
Weight of oil (W) = 49.9 gms
Weight of beads (w) = .0351 gms
$K_{so} = .00364 \frac{W}{w} (D-D_o) = 5.18 (D-D_o)$
Other data same as Run No. 11

April 15, 1955
$\bar{d}_{\frac{3}{2}}$ = 26.6 microns

x	f + c	2R	$\frac{f+c}{R}$	D_o	D	$D-D_o$	K_{so}
36"	10.5"	20mm	26.7	.085	.545	.460	2.38
33	13.5	20	34.3	.08	.548	.468	2.42
30	16.5	20	41.9	.08	.548	.468	2.42
27	19.5	20	49.6	.08	.553	.473	2.45
24	22.5	20	57.2	.083	.558	.475	2.46
20	26.5	20	67.3	.093	.570	.477	2.47
16	30.5	20	77.5	.103	.585	.482	2.50

TABLE 14

Run No. 15
Glass beads in oil
Focal length (f) = 21.0"
Weight of oil (W) = 43.0 gms
Weight of beads (w) = .0309 gms.
Distance of aperture to photocell = 3.4"
Position of collecting lens - 47.2"
$K_{so} = .00364 \frac{W}{w} (D-D_o) = 5.07 (D-D_o)$

April 22, 1955
$\bar{d}_{\frac{3}{2}}$ = 26.6 microns

Aperture dia. (2r) = .0625"

x	f + c	2R	$\frac{f+c}{R}$	D_o	D	$D-D_o$	K_{so}
36"	11.2"	20mm	28.4	.123	.530	.407	2.07
33	14.2	20	36.1	.118	.525	.407	2.07
30	17.2	20	43.7	.110	.520	.410	2.08
27	20.2	20	51.3	.105	.518	.413	2.10
24	23.2	20	58.9	.105	.520	.415	2.11
20	27.2	20	69.1	.105	.523	.418	2.12
16	31.2	20	79.2	.103	.525	.422	2.14
36	11.2	15	38.0	.128	.555	.427	2.16
33	14.2	15	48.1	.125	.548	.423	2.14
30	17.2	15	58.3	.120	.543	.423	2.14
27	20.2	15	68.4	.120	.538	.418	2.12
24	23.2	15	78.6	.120	.538	.418	2.12
20	27.2	15	92.2	.120	.54	.420	2.13
16	31.2	15	106	.120	.543	.423	2.14

TABLE 15

Run No. 16 April 25, 1955
Glass beads in oil $d_{\frac{3}{2}}$ = 26.6 microns
Focal length (f) = 21"
Weight of oil (W) = 51.6 gms Aperture dia. = .105"
Weight of beads (w) = .0379 gms
Position of collecting lens - 47.2"

$K_{so} = .00364 \frac{W}{w} (D-D_o) = 4.95 (D-D_o)$

x	f + c	2R	$\frac{f+c}{R}$	D_o	D	$D-D_o$	K_{so}
36"	11.2"	25mm	22.7	.045	.44	.395	1.96
33	14.2	25	28.8	.045	.44	.395	1.96
30	17.2	25	34.9	.045	.44	.395	1.96
27	20.2	25	41.1	.045	.44	.395	1.96
24	23.2	25	47.2	.045	.445	.39	1.93
20	27.2	25	55.2	.05	.45	.40	1.98
16	31.2	25	63.5	.055	.455	.40	1.98
36	11.2	20	28.4	.045	.44	.395	1.96
33	14.2	20	36.1	.04	.44	.40	1.98
30	17.2	20	43.7	.045	.44	.395	1.96
27	20.2	20	51.3	.045	.445	.40	1.98
24	23.2	20	58.9	.05	.45	.40	1.98
20	27.2	20	69.1	.055	.455	.40	1.98
16	31.2	20	79.2	.065	.465	.40	1.98
36	11.2	15	38.0	.055	.445	.39	1.93
33	14.2	15	48.2	.055	.445	.39	1.93
30	17.2	15	58.3	.06	.45	.39	1.93
27	20.2	15	68.5	.065	.455	.39	1.93
24	23.2	15	78.6	.07	.46	.39	1.93
20	27.2	15	92.3	.08	.47	.39	1.93
16	31.2	15	106	.09	.485	.395	1.96

TABLE 16

Run No. 17 , April 27, 1955
Glass beads in oil
$\bar{d}_{\frac{3}{2}}$ = 26.6 microns
Focal length (f) = 21"
Weight of oil (W) = 51.2 gms
Weight of beads (w) = .0291 gms
Aperture dia. = .105"
Position of collecting lens - 47.2"

$K_{so} = .00364 \frac{W}{w} (D-D_o) = 6.40 (D-D_o)$

x	f + c	2R	$\frac{f+c}{R}$	D_o	D	$D-D_o$	Kso
36"	11.2"	25mm	22.7	.10	.397	.297	1.90
33	14.2	25	28.8	.10	.397	.297	1.90
30	17.2	25	34.9	.10	.395	.295	1.89
27	20.2	25	41.1	.10	.395	.295	1.89
24	23.2	25	47.2	.10	.397	.297	1.90
20	27.2	25	55.2	.10	.40	.30	1.92
16	31.2	25	63.5	.10	.405	.305	1.95
36	11.2	20	28.4	.11	.41	.30	1.92
33	14.2	20	36.1	.11	.41	.30	1.92
30	17.2	20	43.7	.11	.41	.30	1.92
27	20.2	20	51.3	.11	.41	.30	1.92
24	23.2	20	58.9	.11	.412	.302	1.93
20	27.2	20	69.1	.12	.42	.300	1.92
16	31.2	20	79.2	.123	.425	.302	1.93
36	11.2	15	38.0	.125	.435	.31	1.98
33	14.2	15	48.2	.125	.435	.31	1.98
30	17.2	15	58.3	.123	.430	.307	1.96
27	20.2	15	68.5	.123	.430	.307	1.96
24	23.2	15	78.6	.13	.435	.305	1.95
20	27.2	15	92.3	.13	.435	.305	1.95
16	31.2	15	106.0	.14	.445	.305	1.95

TABLE 17

Run No. 20
Glass Beads in oil
Focal length (f) = 20.3"
Weight of oil (W) = 51.8 gms
Weight of beads (w) = .033 gms
Position of collecting lens - 47.4"
Aperture fitted into photocell cover and backed with frosted plexiglass

April 29, 1955
$\bar{d}_{\frac{3}{2}}$ = 26.6 microns
Iris setting 20mm

$$K_{so} = .00364 \frac{W}{w} (D-D_o) = 5.70 (D-D_o)$$

Aperture (2r)	x	f + c	$\frac{f+c}{R}$	D_o	D	$D-D_o$	K_{so}
.0625"	36"	11.4"	29.0	.438	.77	.332	1.89
	27	20.4	51.8	.418	.758	.340	1.94
	16	31.4	79.7	.433	.778	.345	1.97
.105	36	11.4	29.0	.145	.48	.335	1.91
	27	20.4	51.8	.15	.49	.34	1.94
	16	31.4	79.7	.17	.515	.345	1.97
.147	36	11.4	29.0	.12	.445	.325	1.85
	27	20.4	51.8	.12	.45	.33	1.88
	16	31.4	79.7	.135	.475	.34	1.94
.209	36	11.4	29.0	.11	.415	.305	1.74
	27	20.4	51.8	.11	.417	.307	1.75
	16	31.4	79.7	.125	.435	.31	1.77
.297	36	11.4	29.0	.18	.46	.28	1.59
	27	20.4	51.8	.185	.46	.275	1.57
	16	31.4	79.7	.205	.477	.272	1.55
.422	36	11.4	29.0	.180	.41	.23	1.31
	27	20.4	51.8	.185	.417	.232	1.32
	16	31.4	79.7	.205	.437	.232	1.32

TABLE 18

Run No. 21
Glass Beads in oil
Focal length (f) = 20.3"
Weight of oil (W) = 69.2 gms
Weight of beads (w) = .0520 gms
Position of collecting lens - 47.4"
Apertures fitted into photocell cover and backed with frosted plexiglass

April 29, 1955
$\bar{d}_{\frac{3}{2}} = 26.6$ microns
Iris setting (2R) = 20mm

$$K_{so} = .00364 \frac{W}{w} (D-D_o) = 4.84 (D-D_o)$$

Aperture (2r)	x	f + c	$\frac{f+c}{R}$	D_o	D	$D-D_o$	K_{so}
.0400	36"	11.4"	29.0	.275	.695	.42	2.03
	30	17.4	44.2	.31	.715	.405	1.96
	24	23.4	59.4	.327	.727	.400	1.94
	18	29.4	74.6	.335	.743	.408	1.98
.0625	36	11.4	29.0	.055	.475	.42	2.03
	30	17.4	44.2	.065	.485	.42	2.03
	24	23.4	59.4	.08	.495	.415	2.01
	18	29.4	74.6	.11	.52	.41	1.97
.105	36	11.4	29.0	.14	.538	.398	1.93
	30	17.4	44.2	.135	.535	.40	1.94
	24	23.4	59.4	.14	.545	.405	1.96
	18	29.4	74.6	.15	.56	.41	1.98
.147	36	11.4	29.0	.135	.505	.37	1.79
	30	17.4	44.2	.13	.505	.375	1.82
	24	23.4	59.4	.14	.51	.37	1.79
	18	29.4	74.6	.15	.525	.375	1.82
.209	36	11.4	29.0	.07	.420	.35	1.69
	30	17.4	44.2	.075	.42	.345	1.67
	24	23.4	59.4	.08	.425	.345	1.67
	18	29.4	74.6	.085	.435	.35	1.69

TABLE 19

DYNAMIC CALIBRATION DATA

Glass Beads in Air
May 11, 1955

Barometer - 30.70" Hg.
T_{o1} = 73 °F.

Run No.	Bead Feeder Weights (lb.)		TIME Sec.	Manometer Readings (Cm. Hg.)									D_o		D
	Before	After		0	1	2	3	4	5	6	7	Atmos.	Before	After	Mean
1	75.3	65.2	60	5.5	9.9	10.6	11.0	14.5	14.6	14.9	15.0	5.6	.10	.12	.42
2	90.7	83.6	60	5.5	9.8	10.5	10.9	14.3	14.4	14.5	14.6	5.5	.10	.105	.42
3	83.6	75.9	65	5.5	12.8	13.8	14.3	20.2	20.5	20.7	20.6	5.6	.10	.095	.34
4	75.9	69.1	60	5.5	12.8	13.7	14.1	19.6	19.9	20.2	20.4	5.6	.10	.10	.34
5	91.4	85.0	60	5.5	16.0	17.4	17.9	26.8	27.2	27.8	28.2	5.6	.10	.08	.26
6	85.0	78.4	60	5.5	15.9	17.1	17.6	26.7	27.2	27.8	28.2	5.6	.10	.085	.27

APPENDIX I

Sample Calculations

I. Stationary Calibration

Determination of constants for calculation of K_{so} for glass beads suspended in oil:

$$K_{so} = \frac{4}{3}\,\frac{a\,V\rho_b}{w\,l}\,\ln\frac{E_o}{E} \qquad (3)$$

Substituting the equivalents:

$$V = \frac{W}{\rho_{oil}} = \frac{W}{1.076}$$

$$\rho_b = 2.42 \text{ gms/cc}$$

$$l = .995 \times 2.54 = 2.53\text{cm}$$

$$\ln\frac{E_o}{E} = \ln 10 \times \log_{10}\frac{E_o}{E} = 2.3026(D-D_o)$$

$$K_{so} = \frac{4 \times a \times W \times 2.42 \times 2.3026 \times (D-D_0)}{3 \times 2.53 \times 1.076 \times w} = \frac{2.73\ aW(D-D_o)}{w}$$

For d = 26.6 microns:

$$K_{so} = \frac{2.73 \times 26.6 \times 10^{-4}}{2}\,\frac{W}{w}\,(D-D_o) = .00364\,\frac{W}{w}\,(D-D_o).$$

For d = 30.1 microns:

$$K_{so} = \frac{2.73 \times 30.1 \times 10^{-4}}{2}\,\frac{W}{w}\,(D-D_o) = .00411\,\frac{W}{w}\,(D-D_o)$$

With these constants and experimentally observed values of W,w, and $(D-D_o)$, the values of K_{so} may be easily determined.

<u>Dynamic Calibration</u> - Run #5

Mass rate of flow of beads:

Weight of beads and container before run = 91.4 lbs

Weight of beads and container after run = 85.0 lbs

Time for run duration = 60 seconds

$$w_b = \frac{91.4 - 85.0}{60} = .107 \text{ lbs/sec}$$

Mass rate of flow of air:

Pressure at nozzle throat, $p_1 = 67.6$ cm Hg.

Stagnation pressure, $p_o = 78.0$ cm Hg.

$p_1/p_o = .867$

From Gas Tables at $p_1/p_o = .867$:

$M_1 = .456$

$A/A^* = 1.434$

Now

$$\frac{w_a}{A} = \sqrt{\frac{k}{R}}\,\frac{p_o}{\sqrt{T_o}}\left[\frac{2}{k+1}\right]^{\frac{k+1}{2(k-1)}} \cdot \frac{A^*}{A} \tag{G-11}$$

and $T_o = 533^\circ$ R.

$A = \pi/144 \text{ ft}^2$

Solving for w_a:

$w_a = .763$ lb/sec

Velocity of beads at photometer:

$$\left(1+\frac{w_b}{w_a}\right)\frac{V_2^2}{2g} + c_p\,\frac{p_2}{R}\,\frac{A}{w_a}\,V_2 - c_p T_{01} = 0 \tag{G-8}$$

The static pressure at the photometer section,

$$p_2 = 55.8 \text{ cm Hg} = 1552 \text{ lb/ft}^2$$

and $T_{01} = 533^\circ$ R.

$$w_a/A = \frac{.763}{\pi/144} = 35.0 \text{ lb/sec-ft}^2$$

Solving for V_2 directly, $V_2 = 593$ ft/sec

Diameter of Beads:

$$d = \frac{3}{2}\,\frac{K_{so} \times W_b \times L}{A\,V\,\rho_b \times 2.303\,(D - D_0)} \qquad (G-3)$$

where: K_{so} may be assumed equal to 1.975 for the optical system used

l = diameter of test section = 2.0 inches

$A = \pi$ in^2

$\rho_b = 2.42$ gm/cc

$(D-D_o) = .17$ (Observed value)

Substituting these values in equation (G-3), the diameter of the beads may be determined as

$$d = 21.1 \text{ microns.}$$

APPENDIX J

BIBLIOGRAPHY

1. Brillouin, L., "On Light Scattering by Spheres, I", OSRD, Report No. 3038.

2. Brillouin, L. "On Light Scattering by Spheres, II", OSRD, Report No. 3464.

3. Cheatham, J.B., "The Photometric Measurement of Particle Size", M.E. Department, Mech. Eng. Thesis, MIT, 1954.

4. Debye, P.P., "A Photoelectric Instrument for Light Scattering Measurements and a Differential Refractometer", Journal of Applied Physics, 17, May 1946.

5. Gumprecht, R.O., Neng-Lun Sung, J.H. Chin, and C.M. Sliepcevich, "Angular Distribution of Intensity of Light Scattered by Large Droplets of Water", Journal of the Opt. Soc. of Amer., 42, April 1954.

6. Gumprecht, R.O., and Sliepcevich, C.M., "Tables of Light Scattering Functions for Spherical Particles", Eng. Res. Inst., U. of Mich., 1951.

7. "Handbook on Aerosols", Chap. 7, published by AEC, 1950.

8. Houghton, H.G., "Transmission of Visible Light Through Fog", Phy. Rev., 38, 1931, pp 152-158, E.E. Dept. Cont. #74.

9. Houghton, H.G., "The Size and Size Distribution of Fog Particles", Physics, 2, No. 6, June 1932, pp 467-475, E.E. Dept. Cont. #82.

10. Houghton, H.G., "Evaporation of Small Water Drops", Physics, 4, Dec. 1933, pp 419-424.

11. Houghton, H.G., "Research on Fog at the Round Hill Research Station of the Massachusetts Institute of Technology", J. Ae. S., 1, July 1934.

12. Houghton, H.G. and Chalker, W.R., "The Scattering Cross-Section of Water Droplets in Air for Visible Light", Opt. Soc. Amer., 39, 1949, pp 955-957.

13. Humphreys, H.G., "Physics of the Air", McGraw-Hill Book Co, Inc., New York, 1929.

14. Jobst, G., Ann. d. Physik, 76, 1925, p 863.

15. Johnson, J.C., Eldridge, R.G. and Terrell, J.R., "An Improved Infrared Transmissometer for Cloud Drop Sizing", Scientific Report No. 4, Dept. of Meteorology, M.I.T., 1954, July.

16. Johnson, J.C., "Physical Meteorology", John Wiley & Sons, Inc., New York and The Technology Press, M.I.T.; 1954.

17. Keeler, G.E., "Measurement of Droplet Size in an Aerosol by a Modified Impact Probe", thesis for S.M. degree in Mech. Eng., M.I.T., 1954.

18. Keily, D.P., "Measurement of Drop Size Distribution and Liquid Water Content of Natural Clouds", Quarterly Progress Report No. 5, June 1951 to Aug. 1951.

19. Keily, D.P., "Measurement of Drop Size Distribution and Liquid Water Content of Natural Clouds", Quarterly Progress Reports Nos. 1, 2, 3, and 5, Nov. 1950 to Feb. 1951.

20. Kesler, G.H., "Mass Transport in Spray-Laden Turbulent Air Streams", ScD Thesis, Chem. Eng. Dept., M.I.T., 1952.

21. LaMer, V.K. and Sinclair, D., "Verification of the Mie Theory", OSRD Report No. 1857, Dept. of Commerce Off. of Pub. Brd, Report No. 944.

22. LaMer, V.K. and Barnes, M.D., "A Note on the Symbols and Definitions Involved in Light Scattering Equations", Jour. of Colloid Science, 2, 1947.

23. LaMer, V.K. and Barnes, M.D., Journal of Colloid Science, 1, 1946, p 79.

24. McGrew, J. M. "A Study of an Optical Method for Measuring Particle Sizes in Aerosols", S.B. Thesis in Gen. Eng., M.I.T. 1954.

25. Miller, E.P., "Measurement of Particle Size in Aerosols; Collection of Particles", Chem. Eng. Dept. S.M. Thesis, M.I.T., 1953.

26. Mueller, R.H., "Forward Scattering Photometer for Air Pollution Measurement", Analytical Chemistry, 8, Aug. 1954.

27. Nukiyama, S. and Tanasawa, Y., "An Experiment on the Atomization of Liquid by Means of an Air Stream", Trans. S.M.E. (Japan), Vol. 4, Reports 1-6, 1938.

28. Sears, F.W., "Principles of Physics", Vo.III Addison-Wesley Press, Inc. Cambridge, Mass. 1948.

29. Shapiro, A.H., Wadleigh, K.R., Gavril, B.D., and Fowle, A.A., "The Aerothermopressor-A Device for Improving the Performance of a Gas Turbine Power Plant".

30. Sinclair, D., and Lamer, V.K., "Light Scattering as a Measure of Particle Size in Aerosols", Chemical Reviews, 44,1949.

31. Sinclair, D., "Measurement of Average Particle Size in Aerosols by Light Scattering", ASME Paper No. 55-APC -10.

32. Sinclair, D., "Light Scattering by Spherical Particles", Jour. Opt. Soc. of Amer., 37, June 1947.

33. Stern, H., "Investigation of a Method to Determine Particle Size in Aerosols", M.E. Dept., S.M. Thesis, M. I. T. 1951.

34. Stratton, J.A., "Electromagnetic Theory", McGraw-Hill Book Co. Inc., New York 1941, p 563-567.

35. Stratton, J.A. and Chu, L.J., "Diffraction Theory of Electromagnetic Waves", Phy. Rev., 56, 1939, E.E. Dept. Cont. #169.

36. Stratton, J.A. and Houghton, G.H., "Theoretical Investigation of the Transmission of Visible Light Through Fog", Phy. Rev., 38, 1931, pp 159-165, E.E. Dept. Cont. 74.

37. Shapiro, A.H., "The Dynamics and Thermodynamics of Compressible Fluid Flow", Ronald Press, New York, 1953.

38. Keenan, J.H. and Kaye, J.,"Gas Tables", John Wiley and Sons, New York, 1948.

39. Gottling, P.F., "Development of an Impact Probe for Determining Droplet Size in Aerosols",S.M. thesis in preparation, Mech. Eng.Department, M.I.T., June 1955.

Thesis 28917
B168 Baker
The photometric measurement
of droplet size.